Central Australian Cold Fronts

ROGER K. SMITH

Meteorological Institute, University of Munich, Munich, Germany

MICHAEL J. REEDER

Centre for Dynamical Meteorology and Oceanography, Monash University, Melbourne, Victoria, Australia

NIGEL J. TAPPER

Department of Geography and Environmental Science, Monash University, Melbourne, Victoria, Australia

DOUGLAS R. CHRISTIE

Research School of Earth Sciences, Australian National University, Australia

(Manuscript received 16 September 1993, in final form 4 April 1994)

ABSTRACT

This paper presents an observational study of the structure and behavior of cold fronts over central Australia during the late dry season, a time of year when the prefrontal convectively well-mixed layer is particularly deep. The study is based on the results of the Central Australian Fronts Experiments (CAFE) held in 1991. Three fronts were documented in unprecedented detail for the Australian region using a greatly enhanced surface-observing network and a boundary layer wind profiler, as well as serial upper-air soundings. Data on the surface energy balance were obtained also.

A common feature of the fronts observed during CAFE was that they were dry, shallow (~1 km deep), and moved into a deep (~4 km) convectively well-mixed boundary layer. One of them initiated major dust storms across central Australia. A prominent feature of the fronts was the marked diurnal variation of their surface signature as they moved through the network. Noteworthy was the tendency during the night for the initiation in the accompanying trough of undular borelike structures or other nonlinear wave disturbances that moved ahead of the main airmass change. One well-documented case illustrates the generation of a southerly morning glory bore wave in the southern Gulf of Carpentaria region. During the daytime, fronts over central Australia are difficult to locate from surface data and appear to decelerate and to weaken greatly. Some dynamical aspects of the observations are discussed.

1. Introduction

The impetus for the present study originated in attempts to explain the origin of certain nocturnal wind surges observed in the southeastern part of the Gulf of Carpentaria region of northern Australia. On occasion these wind surges lead to spectacular cloud formations known locally as "morning glories." They are also of fundamental meteorological interest, being the example, par excellence, of an undular bore wave disturbance in the lower atmosphere, the atmospheric equivalent of undular bores on tidal rivers. Their occurrence poses a significant analysis problem in the data-sparse region of northwestern Queensland (Smith et al. 1986). Up-to-date reviews are to be found in Smith (1988) and Christie (1992).

Morning glory wind surges originate predominantly from two directions: from the northeast and from the south. Research during the last decade has shown that northeasterly wind surges are generated by the collision of the east and west coast sea breezes over Cape York Peninsula (see, e.g., Clarke et al. 1981; Noonan and Smith 1987), but the generation mechanism for southerly surges remains uncertain. Physick and Tapper (1990) have shown that the large salt lakes of central Australia are possible sources of solitary wave–type disturbances, while katabatic drainage has been implicated also (Clarke 1972). Nevertheless, there is strong circumstantial evidence that most southerly wind surges are associated with the passage of cold fronts across central Australia (Christie et al. 1981; Smith et al. 1986; Smith and Ridley 1990).

Corresponding author address: Prof. R. K. Smith, Meteorological Institute, University of Munich, Theresienstr. 37, 80333 Munich, Germany.

Attempts to establish a clear link between southerly wind surges and cold fronts raise fundamental questions concerning the structure and dynamics of subtropical continental cold fronts themselves. We soon came to realize that this is a subject of considerable relevance to the meteorology of the Australian tropics in its own right, but one that has received relatively little attention by researchers until recently. This is despite the difficulties encountered in analyzing such fronts over central and northern Australia. One difficulty, of course, is that the routine data network is totally inadequate for a proper study and is rarely adequate even for the analysis of synoptic fronts. The behavior of continental cold fronts in the dry subtropics is of intrinsic scientific interest also because they move into an air mass that is convectively well mixed through a considerable depth, typically 3–4 km over central and northern Australia in the late dry season.

The Central Australian Fronts Experiment (CAFE) was organized to provide a dataset on subtropical cold fronts that could be used to answer some of the basic questions about frontal structure and behavior, and to confirm or reject predictions provided by future model simulations. The experiment ran from 7 September until 4 October 1991 and documented three cold fronts in considerable detail. As a preliminary to this, a rather modest pilot experiment was organized in September 1988 to investigate the vertical structure of cold fronts as they passed over Mount Isa (21°S, 139°E). We shall refer to this as the pre-CAFE experiment. Three frontal passages were documented during pre-CAFE also and the results were reported by Smith and Ridley (1988).

The present paper contains an analysis of findings from CAFE, highlighting common features of the fronts observed. It is organized as follows. The objectives and network design of CAFE are described in section 2. Section 3 presents a synoptic overview of the three CAFE events. Mesoscale aspects and the vertical structure of the CAFE fronts are considered in section 4. Section 5 contains a brief analysis of surface flux data during frontal passages. Theoretical issues are raised in section 6 and this is followed in section 7 with the conclusions, which include a summary of the principal characteristics of fronts studied.

2. CAFE: Aims and experimental design

Two major aims of the CAFE experiment were

(i) to investigate the structure and behavior of subtropical cold fronts that affect central and northeastern Australia;

(ii) to investigate the interaction of subtropical cold fronts with the developing nocturnal inversion and the generation of propagating borelike or solitary wave disturbances.

Accordingly, the experiment was designed to provide a greatly enhanced surface data network, in particular to the southwest, to the east, and to the north of Mount Isa. This network, together with the orography of the region, is shown in Fig. 1. Two types of station were installed: a series of 10 fully automated stations recording wind speed, wind direction, wet-bulb temperature, dry-bulb temperature, and pressure; and 12 high-resolution micropressure and temperature recording stations. In addition, a full energy balance station was established at Hughenden to enable the measurement of radiative, sensible, and evaporative heat fluxes during the passage of fronts.

The operations center was located at the Bureau of Meteorology Mount Isa Office, which is a routine upper-air station and where the normal facilities of a forecast office were available. Two extra upper-air stations were established at Hughenden and Burketown using Väisälä Marwinsonde equipment and additional upper-air soundings were made at the bureau stations at Alice Springs and Mount Isa, prior to and after frontal passages.

An important facility available to the experiment was the microwave (914 MHz) boundary layer wind profiler operated by Mount Isa Mines Ltd. (Restall and Shyu 1991). The profiler provided three-dimensional wind fields up to a height of 3–4 km, depending on conditions, with a vertical resolution of about 100 m. Soundings of this type were available as averages every 5 min.

3. A synoptic overview of the CAFE cold fronts

To set the scene for the analysis of frontal structure and evolution in the next section, we review the broad-scale synoptic settings for the three cold fronts that were documented during the CAFE experiment, henceforth referred to as CE1, CE2, and CE3.

The mean sea level pressure (MSLP) and the 1000-mb dry-bulb and wet-bulb potential temperature analyses presented have been constructed objectively using the Bureau of Meteorology analysis scheme. The latter is part of a limited-area assimilation system that has a horizontal resolution of 150 km; it is described by Mills and Seaman (1990). In this paper we will define the *front* by the axis of maximum relative vorticity. This definition is consistent with the modeling results of Reeder and Smith (1988) and Reeder et al. (1991), who showed that the axis of maximum relative vorticity provides a robust indicator of frontal position even in the presence of strong differential surface heating. For the most part, this definition is consistent with common usage; as may be seen in the synoptic analyses discussed below, in central and northern Australia, the axis of maximum relative vorticity roughly marks the leading edge of the airmass change. In the southern part of the continent, the airmass change is less well defined than in the north and the relative vorticity axis provides an objective means of defining the (albeit weak) southern part of the front. In addition to the fronts as defined

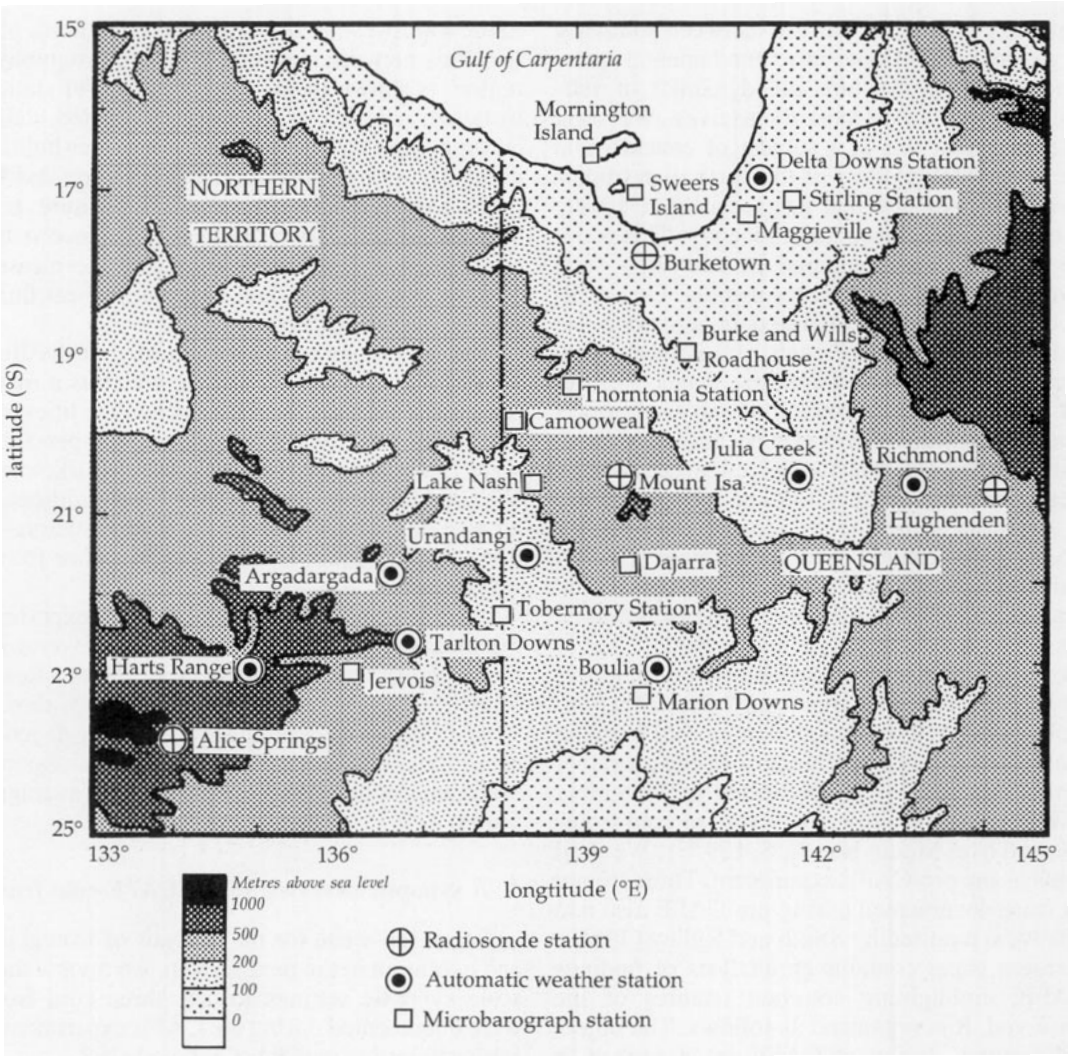

FIG. 1. Map showing the orography and the distribution of stations in the CAFE network.

above, the axes of maximum relative vorticity associated with the two heat troughs in the northern part of the continent (the Western Australian and Queensland heat troughs) are shown on the MSLP analyses. As discussed below, it would appear that the horizontal temperature gradients associated with these heat troughs provide the background field for frontogenesis in the Australian subtropics.

a. Event 1

This cold front was associated with a low pressure system that originated as a secondary development, that is, a frontal wave, on a long northwest–southeast-oriented cold front that, traveling northeastward, crossed the southwestern corner of the Australian continent at about 0600 EST[1] 8 September 1991. The following day, at 2100 EST, the low had deepened and was centered just south of Adelaide at approximately 36°S, 137°E, and the axis of maximum relative vorticity was analyzed to lie along a line extending approximately in a north-northeasterly direction from the low (Fig. 2a). Much farther east, an anticyclone over the Tasman Sea extended a broad ridge along the east coast of Australia, although pressure gradients over much of eastern Australia were generally weak. A pronounced trough extended from the surface low located just to the south of the continent through to the northeastern corner of Western Australia.

The northern part of the trough was associated with prominent maxima in the 1000-mb potential temperature (Fig. 2b), and in the cyclonic relative vorticity (Fig. 2a). Such low-level temperature maxima arise through differential daytime heating and orographic effects and are common features of the analyses at this time of the year (Fandry and Leslie 1984; Adams 1986;

[1] Australian eastern standard time is UTC + 10 h.

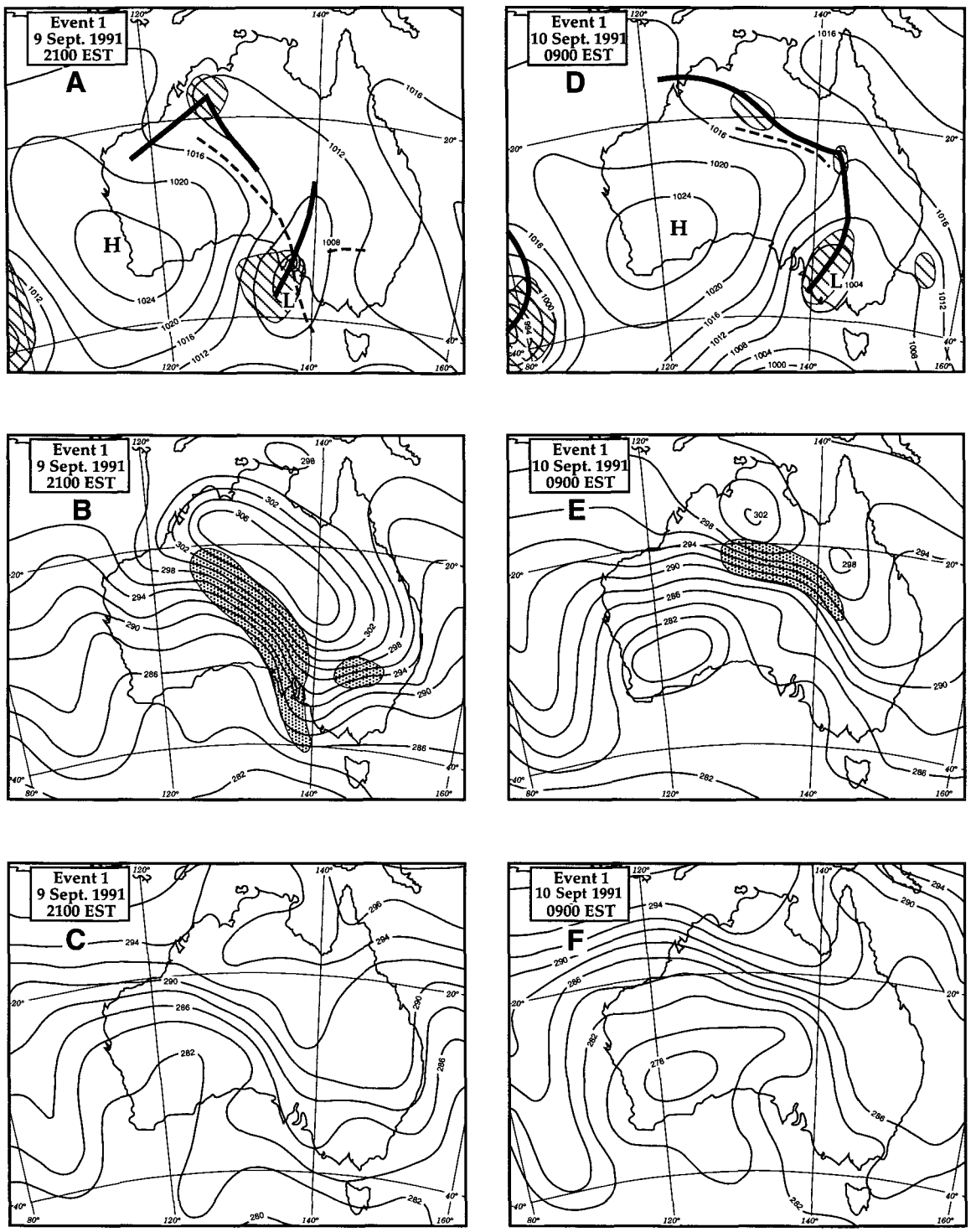

FIG. 2. Australian Bureau of Meteorology objective analyses showing the synoptic conditions for CAFE event 1. (a) Mean sea level pressure, (b) 1000-mb dry-bulb potential temperature, and (c) 1000-mb wet-bulb potential temperature for 2100 EST 9 September. (d) Mean sea level pressure, (e) 1000-mb dry-bulb potential temperature, and (f) 1000-mb wet-bulb potential temperature for 0900 EST 10 September. Shown also in panels (a) and (d) are the axes of maximum relative vorticity associated with the two heat troughs in the northern part of the continent; the regions in which the cyclonic relative vorticity as *analyzed* on a 150-km resolution grid exceeds 4×10^{-5} s^{-1}; and the axis of maximum temperature gradient at 950 mb. The shaded areas in panels (b) and (d) are where the potential temperature gradient exceeds 2 K $(100\ km)^{-1}$.

Leighton and Deslandes 1991; Kepert and Smith 1992). Note that the strongest potential temperature gradients, highlighted by the shaded region in Fig. 2b, occurred on the southwestern flank of the heat trough. The wet-bulb potential temperature (Fig. 2c) is less sensitive to diurnal variation in the surface sensible heating and provides a good indicator of the airmass change.

At 0900 EST 10 September, the parent low had deepened further and its center now lay near 36°S, 142°E. The relative vorticity axis associated with the low had moved farther eastward and appeared in the Bureau of Meteorology objective analysis to be *southeast* of Mount Isa where its orientation was almost north–south (Fig. 2d). At this time, as shown by the cyclonic relative vorticity maxima in Fig. 2d, the Western Australian heat trough had become displaced several hundred kilometers eastward and was part of a northwest–southeast-oriented front, as defined by the axis of maximum relative vorticity, just to the southwest of Mount Isa. Figure 2f shows that a pronounced airmass change accompanied the passage of the front through the CAFE network. In contrast, the airmass change was poorly defined in the south of the continent. At about 0930 EST, the trough line crossed Mount Isa, accompanied by strong squally winds and blowing dust, which severely reduced visibility for the following 8 h and necessitated the closure of Mount Isa airport for a period. Strong ridging occurred behind the airmass change as it advanced across the CAFE network. During the day the airmass change appeared to stall to the east of Mount Isa. Subsequently, the change accelerated during the early evening, reaching Hughenden at about 2030 EST. The front–trough system crossed the entire CAFE surface network in under a day, the western section between Alice Springs and Mount Isa during the night and early morning, the eastern section between Mount Isa and Hughenden during the daytime and early evening.

b. Event 2

The synoptic situation had many similarities with that of CE1. Again the low with which the cold front was associated formed as a secondary development on a long northwest–southeast-oriented front as the latter approached the continent from the Southern Ocean, southwest of Western Australia. At 0900 EST 15 September, the low center was situated at approximately 40°S, 121°E with its cold front again trailing to the northwest over the southwest corner of Western Australia. In the following 24 h the low center and its associated cyclonic vorticity maximum had moved eastward to about 39°S, 132°E, and the cold front was analyzed to have just entered the southwest corner of the Northern Territory, some 300 km southwest of Alice Springs. Twelve hours later, at 2100 EST 16 September, the cold front was analyzed to be *southeast* of Mount Isa (Figs. 3a–c). On the other hand, the trough extending between the two northern cyclonic relative vorticity maxima, which characterize the Western Australian and Queensland heat lows, was oriented northwest–southeast and over western Queensland lay to the southwest of Mount Isa. As shown in Fig. 3c, the airmass change was positioned southwest of Mount Isa at this time also. In common with the first event, in the northern part of Australia the trough was associated with a pronounced maximum in the 1000-mb potential temperature (Fig. 3b). Later that night, at 0020 EST the front passed through Mount Isa where the winds veered sharply from a 3–4 m s^{-1} northerly to a gusty southerly of around 5–10 m s^{-1}. The following morning at 0900 EST 17 September, the cold front was analyzed at the eastern limit of the CAFE network, to the east of Hughenden (Figs. 3d–f). The airmass change, as reflected in the wet-bulb potential temperature, penetrated into northern parts of the CAFE network (Fig. 3f). In contrast to CE1, CE2 crossed the western part of the CAFE network during the daytime and early evening and the eastern part during the night and early morning.

c. Event 3

This event began in a similar way to the two earlier ones, the main differences being that secondary development on the existing front did not occur until the front was already over South Australia, and the strength of the ridging behind the front was comparatively weak. The Bureau of Meteorology objective analyses for 2100 EST 1 October 1991 are shown in Figs. 4a–c. A prominent feature of the analysis is the Western Australian heat trough, which is highlighted by the shaded region in Fig. 4a. At this time the northernmost part of the cyclonic vorticity axis associated with the extratropical low, that is, the analyzed front, lay some 200 km southwest of Alice Springs. The situation one day later is shown in Figs. 4d–f. At this time the low had stalled over western New South Wales; its central pressure was unchanged from the previous day, and the front weakened. This pattern remained more or less stationary throughout the following day with the ridge to the west of the low steadily extending northward. Thereafter, the pressure gradients weakened in situ. While weaker in northern Australia than the first two events, the mesoscale aspects of this front over the eastern part of the CAFE network are of interest and are described in detail in section 4.

d. Summary and comparison with the pre-CAFE fronts

The synoptic analyses presented in Figs. 2–4 show that the subtropical part of the front was fundamentally different in character to that in the southern part of the continent, and to some extent, these were independent

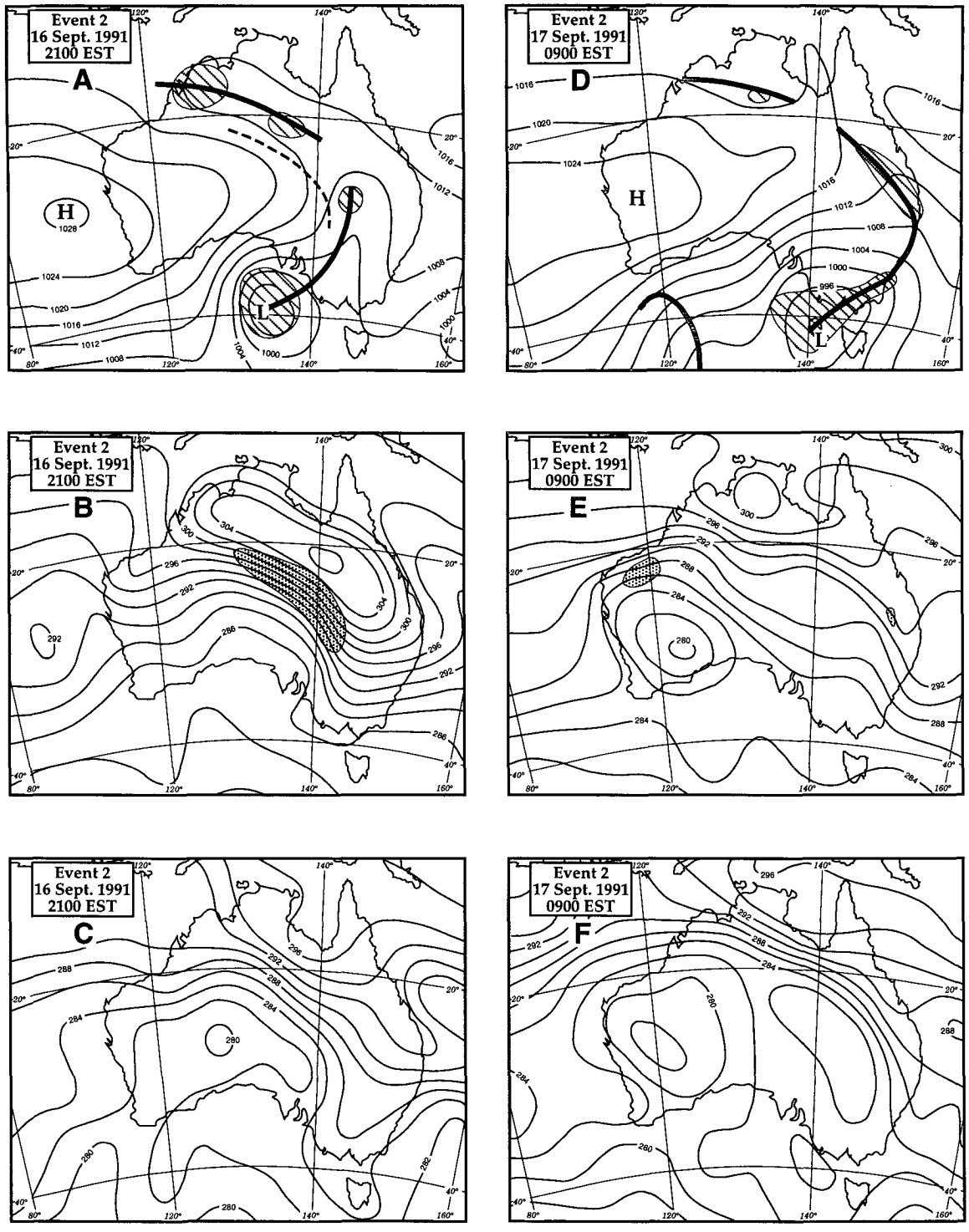

FIG. 3. Australian Bureau of Meteorology objective analyses showing the synoptic conditions for CAFE event 2. (a) Mean sea level pressure, (b) 1000-mb dry-bulb potential temperature, and (c) 1000-mb wet-bulb potential temperature for 2100 EST 16 September 1991. (d) Mean sea level pressure, (e) 1000-mb dry-bulb potential temperature, and (f) 1000-mb wet-bulb potential temperature for 0900 EST 17 September 1991. Legend otherwise as in Fig. 2.

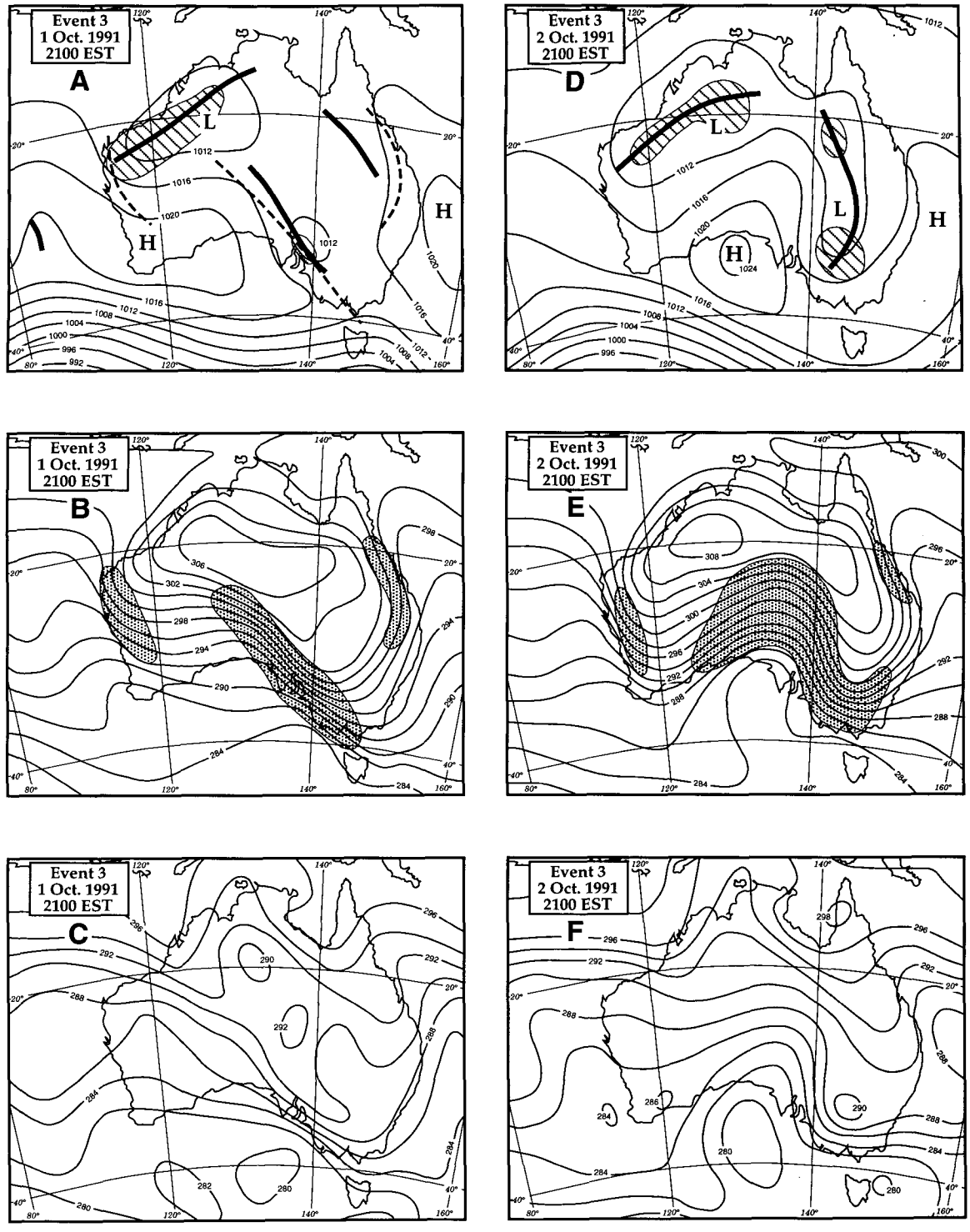

FIG. 4. Australian Bureau of Meteorology objective analysis showing the synoptic conditions for CAFE event 3. (a) Mean sea level pressure, (b) 1000-mb dry-bulb potential temperature, and (c) 1000-mb wet-bulb potential temperature for 2100 EST 1 October 1991. (d) Mean sea level pressure, (e) 1000-mb dry-bulb potential temperature, and (f) 1000-mb wet-bulb potential temperature for 2100 EST 2 October 1991. Legend otherwise as in Fig. 2.

of each other. In particular, in the subtropics, the front appeared to be closely tied to the heat trough and was accompanied by a pronounced change in the air mass. Another distinguishing feature was the strong ridging and cold-air advection that accompanied the subtropical airmass change. Conversely, the extratropical front was characterized by a weak airmass change and its motion appeared to be linked closely to that of the extratropical cyclone.

The broad-scale synoptic conditions for CE1 and CE2 were similar to those that occurred during pre-CAFE, the most notable difference being that the parent lows developed much closer to the continent. During pre-CAFE, the parent low centers were all poleward of 48°S. In all these five cases, strong postfrontal ridging occurred over central Australia, and the systems remained mobile, traversing the entire continent. In CE3 the ridging was weaker and more localized and the whole system stagnated and decayed over the continent.

4. Mesoscale aspects of frontal evolution

In each of the three CAFE events, at least after sunset, a marked pressure disturbance was observed to preceed the airmass change, the main exception being at Harts Range during CE1 (see below). During the day, however, at least from late morning to around sunset, it was difficult to identify the frontal passage from the surface data. A notable difference between the two strong frontal systems, CE1 and CE2, was the different time of day that their leading edge passed a particular station, a difference typically of 9 h. This had clear implications with regard to the frontal structure, which in both cases underwent a significant *diurnal* variation. Again we consider briefly each event in turn.

a. Event 1

This passed through Alice Springs at 2355 EST 9 September at which time there was an abrupt wind shift from the west to south-southwest, an abrupt increase in surface wind speed, a small temperature rise (about 1°C), and a pressure jump of about 0.5 mb. Radiosonde soundings at Alice Springs airport at 2100 EST 9 September about 2 h before the passage and at 0900 EST, some 10 h after the event, showed appreciable cooling in the lowest 2.5 km above ground level (AGL)—indeed, over 15°C in the lowest kilometer (Fig. 5). Such cooling is consistent with the synoptic analyses of potential temperature at 2100 EST 9 September and 0900 EST the next day displayed in Figs. 2b and 2e. The mixed-layer depth before the arrival of the front was over 3 km AGL. The frontal zone moved northeastward, the leading pressure jump reaching Mount Isa at 0930 EST 10 September. However, the pressure jump was difficult to identify from surface data north of Thorntonia Station (1043 EST) and to the east of

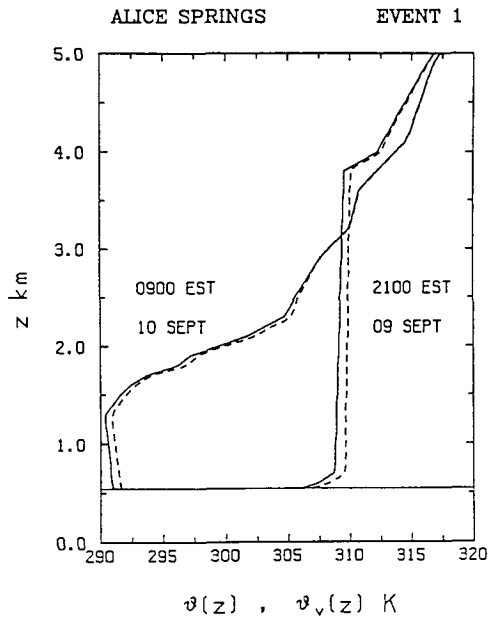

FIG. 5. Vertical profiles of potential temperature and virtual potential temperature, $\theta(z)$ and $\theta_v(z)$, in the prefrontal and postfrontal air mass at Alice Springs for the first event during CAFE. The frontal passage at Alice Springs occurred at 2355 EST 9 September.

Julia Creek (1143 EST), that is, during the late morning and afternoon when there was strong convective heating. Later, in the evening (2020 EST), the airmass change was observed to pass through Hughenden.

The nocturnal evolution is of particular interest. At Harts Range (Fig. 6), some 300 km northeast of Alice Springs, the frontal passage at 0225 EST was characterized at the surface by a single change marked by a sudden increase in wind speed from almost calm conditions, a change in wind direction, and a sharp temperature rise (~7°C), but heralded only a gradual rise in pressure with no pressure jump. The abrupt temperature rise, associated with the destruction of a shallow radiation inversion by downward mixing, was followed by a steady decrease in temperature, the rate being -2.5°C h^{-1} for two hours after the change. Although this rate is similar to the rate of nocturnal cooling before the disturbance passage, the latter occurred under calm wind conditions with the cooling being confined presumably to a shallow layer. It is reasonable to assume that this rate could not be maintained under strong wind conditions without cold-air advection. At Tarlton Downs (Fig. 7) the frontal passage was marked by an abrupt pressure jump of about 1.5 mb at 0405 EST, but there was evidence that the airmass change occurred at around 0440 EST, at which time the temperature began to fall steadily at the rate -2.8°C h^{-1} similar to the slow decrease at Harts Range following the initial sharp rise. Again this occurred under strong wind conditions and cannot all be attributed to nocturnal cooling. At Arga-

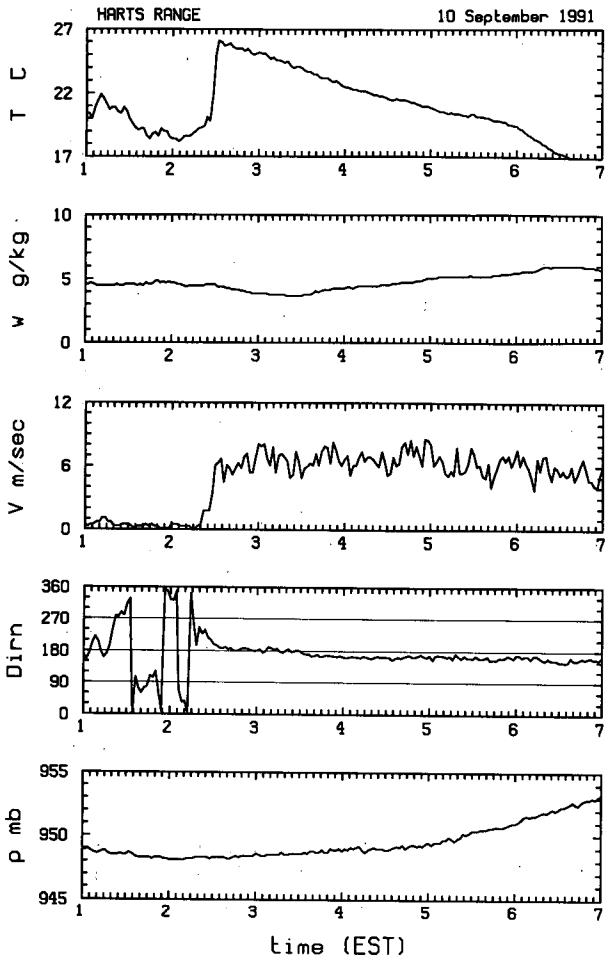

FIG. 6. Surface station data at Harts Range surrounding the passage there of the first front during CAFE. (a) Temperature; (b) mixing ratio; (c) wind speed; (d) wind direction; and (e) pressure.

dargada (Fig. 8), the main pressure jump at about 0555 EST was marked by a significant southerly wind surge. The airmass change occurred about 20 min later as shown by the onset of a second wind surge and sudden decrease in surface mixing ratio at 0615 EST. There is evidence also of another smaller amplitude pressure disturbance at about 0510 EST, some 65 min ahead of the airmass change. At Urandangi the front had a conspicuous double structure also. There the leading change at 0700 EST was characterized by a pressure jump (~1.8 mb) and a sharp change in wind direction, followed by a series of pressure waves that coincided with fluctuations in the wind speed and direction (Fig. 9). These observed wind and pressure signatures are typical of those associated with an amplitude-ordered family of solitary waves (Smith 1988; Christie 1992). As a moderate northwesterly wind was blowing before the disturbance arrived, the temperature *rise* accompanying these waves was relatively small (<1°C). The second change, at 0815 EST, marked the airmass boundary and was accompanied by a strong surge in the wind (~10 m s^{-1}), a further wind direction change, a sharp decrease in dewpoint temperature and mixing ratio, and a further jump in pressure, albeit smaller than with the leading change.

As CE1 crossed the network, detection of the cold airmass boundary was obscured at all stations except Jervois by the downward mixing of potentially warmer air from above the nocturnal inversion. Time series from the high-resolution micropressure and temperature station at Jervois, which lies in the southwestern corner of the network, are shown in Fig. 10. There, the passage of the pressure disturbance was accompanied by a sudden decrease in temperature of about 1°C followed by a gradual temperature decrease at a rate of about 2.6°C h^{-1}, suggesting that during the early stages of CE1, the airmass boundary and the pressure disturbance were coincident.

The radical evolution in frontal structure from a single to a double change is similar to the behavior of a gravity current as it moves into a shallow surface-based, stably stratified layer. If the stable layer is sufficiently deep in relation to the depth of the gravity current, a nonlinear wave disturbance forms and propagates ahead of the gravity current. If the stable layer

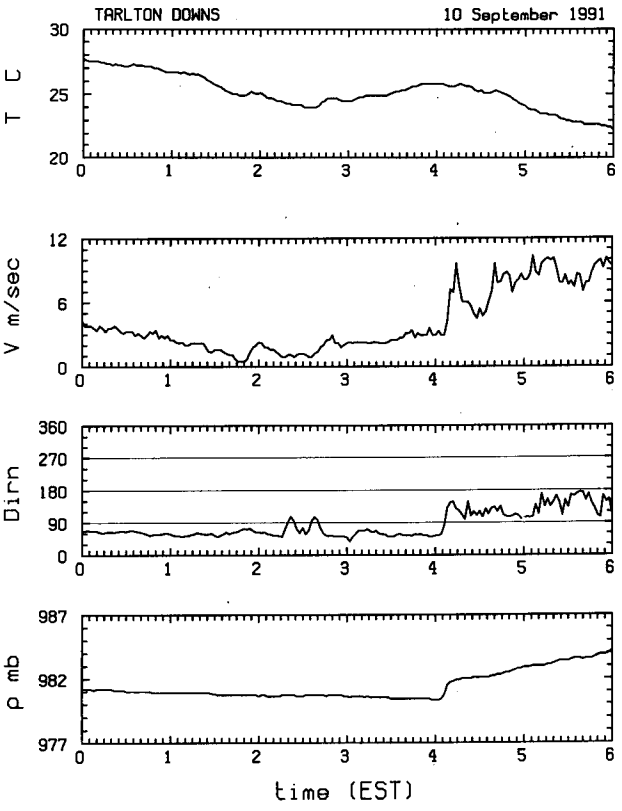

FIG. 7. Surface station data at Tarlton Downs surrounding the passage there of the first front during CAFE. (a) Temperature; (b) wind speed; (c) wind direction; and (d) pressure (mixing ratio data were unavailable).

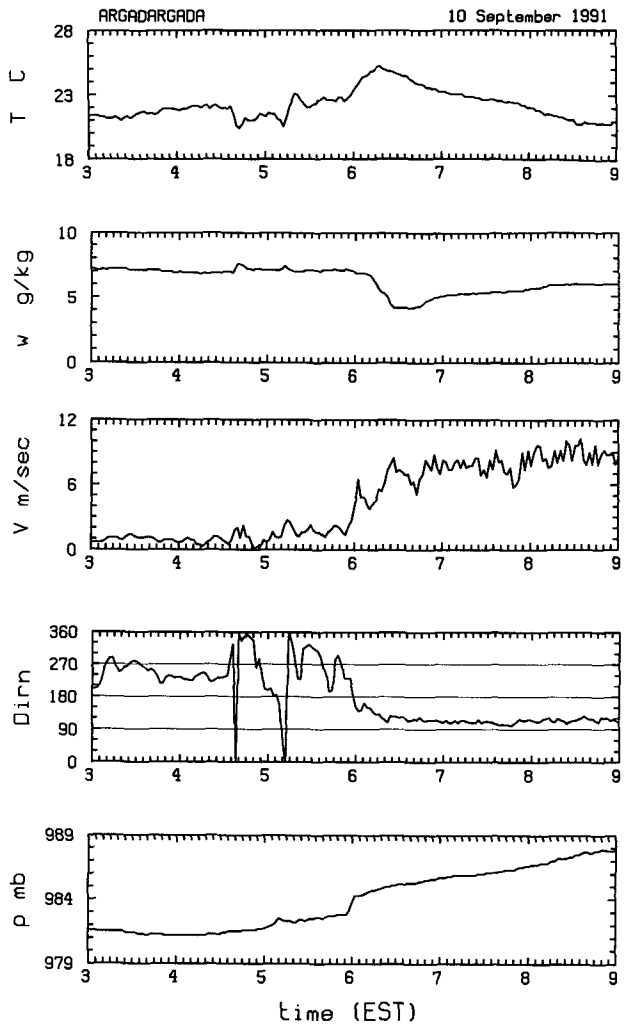

FIG. 8. Legend as for Fig. 6 except for Argadargada.

is too shallow for this to happen, the presence of the stable layer has a profound effect on the structure of the gravity-current head, which develops one or more large-amplitude waves enveloping colder air (Wood and Simpson 1984; Rottman and Simpson 1989; Haase and Smith 1989). However, our data are inadequate to determine the extent to which gravity current dynamics are locally applicable to the front, or which, if either, of the two foregoing scenarios is most relevant to the observed fronts (see section 6).

The development of a series of solitary waves ahead of the main airmass change is shown also by the time series of surface pressure obtained from the microbarograph stations in Fig. 11. Prefrontal waves first appeared in the pressure signature at Tobermory Station (0530 EST) and continued to develop as the disturbance propagated over Dajarra (0748 EST), Lake Nash (0847 EST), and Camooweal (1000 EST). It is interesting to note that the amplitude of the leading waves increases substantially as the disturbance evolves in agreement with the predictions of nonlinear dispersive wave theory (Christie 1989).

The anemograph trace at Mount Isa showed a series of peak wind gusts separated by lulls with a period of 10 to 15 min. These were accompanied by a corresponding fluctuation in the wind direction as the wind turned from a northwesterly to a southwesterly. At about the same time there was a pressure jump of approximately 1 mb, but as the time resolution of the barograph was poor, it was not possible to determine whether there were oscillations in the surface pressure. The behavior was similar to that at Urandangi (see Fig. 9), where the wind fluctuations had a similar period, and is consistent again with a series of solitary waves ahead of the front. The fluctuations in wind speed and direction are clearly evident in the low-level wind vectors shown in Fig. 12, constructed from the Mount Isa Mines wind profiler data. They began at 0945 EST and continued until at least 1015 EST extending to just under 1 km AGL. Above this height the winds remained

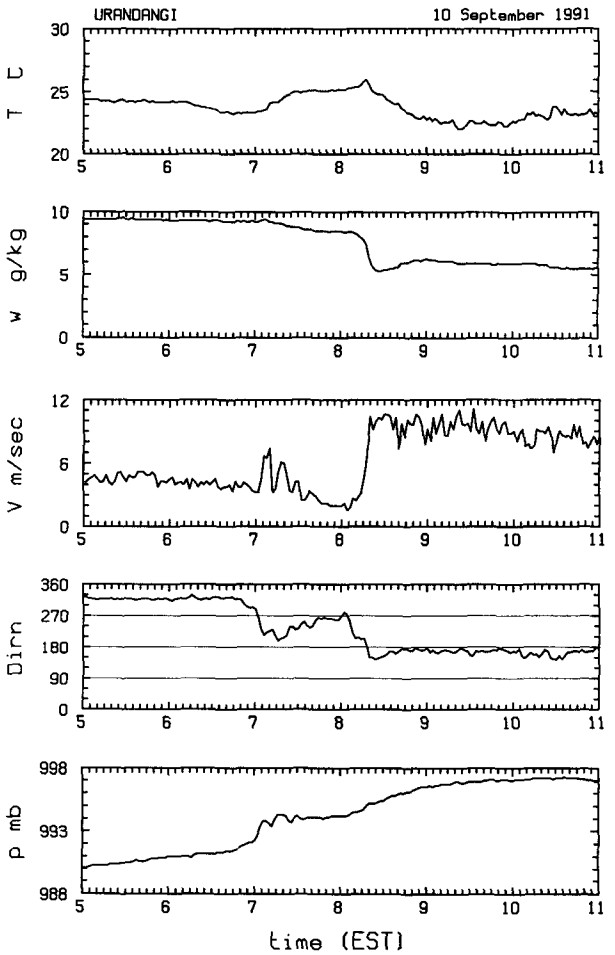

FIG. 9. Legend as for Fig. 6 except for Urandangi.

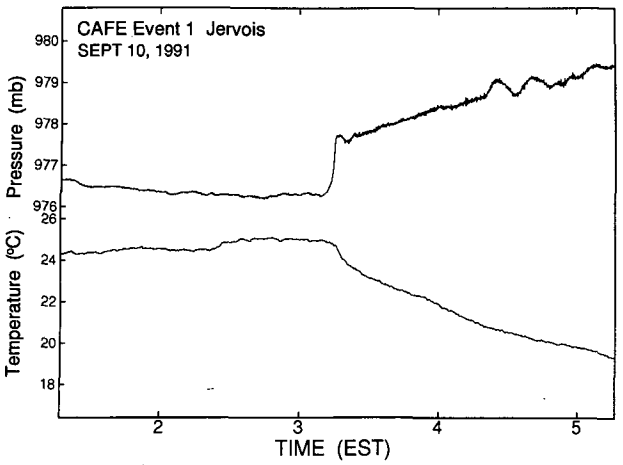

FIG. 10. Time series from the micropressure and temperature station at Jervois surrounding the passage of the first CAFE event.

northwesterly. Note that the profiler winds are averaged over 5-min intervals, just sufficient to resolve the waves.

Figure 13 shows the *NOAA-12* Advanced Very High Resolution Radiometer (AVHRR) satellite image at 0818 EST 10 September 1991. At this time the change was still to the southwest of Mount Isa. A spectacular rope cloud embedded within a broader cloud band is evident in the image. The rope cloud marks the leading edge of the pressure jump rather than the leading edge of the cold air mass.

It is to be expected that the airmass change and preceeding pressure disturbances were undergoing rapid modification in the Mount Isa region as the early morning low-level radiation inversion was removed by renewed convective mixing. Changes in the static stability during an 18-h interval surrounding this transition period are characterized by the vertical profiles of virtual potential temperature $\theta_v(z)$ shown in Fig. 14. These profiles are based on radiosonde soundings at Mount Isa at 2100 EST 9 October and at 0600, 0900 (40 min before the arrival of the front), 1200 and 1500 EST 10 October. It is reasonable to assume that the first three of these soundings are typical of the prefrontal air mass in a region of at least 100 or 200 km around Mount Isa including the nearby microbarograph and surface stations in our network. Just before sunrise there was a strong stable layer about 500 m deep underlying a much deeper layer of low static stability extending to 3.8 km AGL. Before the arrival of the leading change at Mount Isa, the stable layer had been removed and replaced by a mixed layer some 700 m deep, which was capped by a strong inversion. The two postfrontal soundings show cooling extending to 2.8 km AGL, but with the major cooling below about 1.7 km AGL. The mixed-layer depth by midafternoon on 10 September was only about 1.5 km, compared with 3.2 km on the previous day.

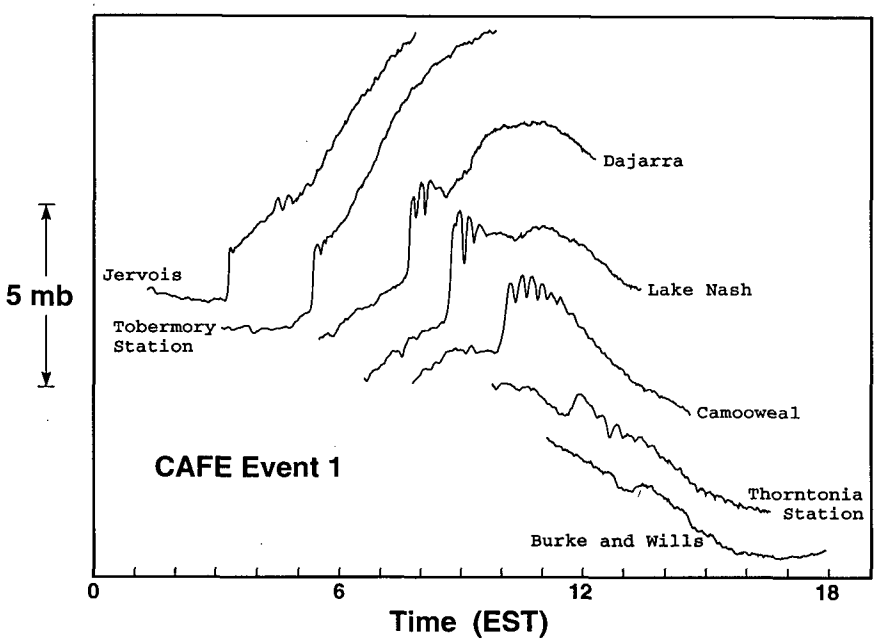

FIG. 11. Surface pressure signatures recorded at microbarograph stations at and to the south of Burke and Wills Roadhouse during the first CAFE event. The signatures are arranged sequentially with the southwesternmost station (Jervois) at the top and northeasternmost (Burke and Wills) at the bottom. Note the development of a wavelike signature as the disturbance moves northeastward, prior to its demise northeast of Camooweal.

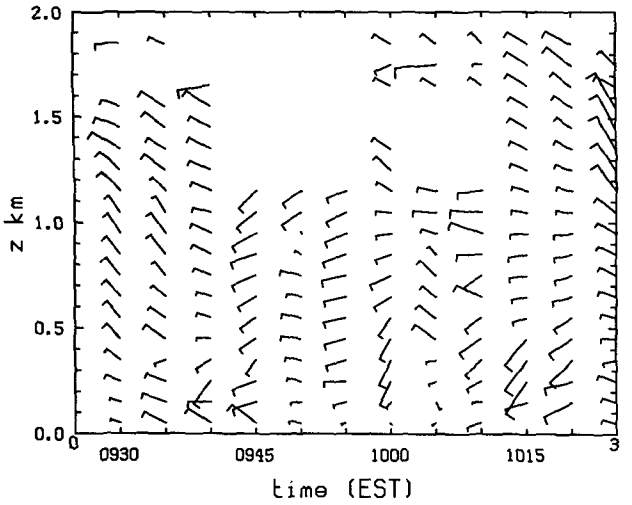

FIG. 12. Time–height display of horizontal wind vectors based on data obtained from the Mount Isa wind profiler during the passage of the first CAFE event. The first coherent onset of southwesterly winds is seen at 0945 EST and extends to a little over 1 km AGL. The second onset occurs at 1000 EST but is shallower, and the third occurs at 1010 EST. Wind vectors are scaled so that 5 min along the abscissa corresponds with a wind speed of 20 m s^{-1}.

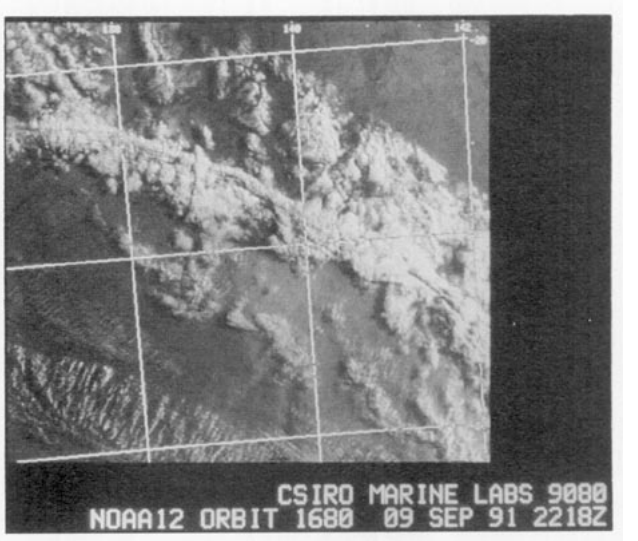

FIG. 13. *NOAA-12* AVHRR visible satellite image at 0818 EST 10 September 1991.

The isochrones of the pressure jump for this event, shown in Fig. 15a, indicate a steady movement of the leading edge of the disturbance with a speed of 15.0 ± 0.2 m s^{-1} between Harts Range and Mount Isa. In the region south of Argadargada the motion was from a direction of 195°. To the northwest of Mount Isa, between Camooweal and Thorntonia Station, the speed was slightly lower, about 13.0 ± 0.2 m s^{-1}. A relatively weak disturbance evident in the surface pressure field continued to propagate northward during the afternoon. This accelerated slightly, reaching a speed of about 16.5 ± 0.2 m s^{-1} over the southern margin of the Gulf of Carpentaria. At Harts Range, the airmass boundary appeared to coincide with the leading pressure jump as described above. However, it decelerated as it moved northeastward allowing the wave disturbance to move out ahead of it as an essentially independent disturbance (Fig. 16). The average speed of the airmass boundary between Harts Range and Camooweal was about 10 m s^{-1}. It could not be detected at stations north of Camooweal. The frontal passage became increasingly difficult to locate during the daytime at surface stations to the east of Mount Isa also. At Julia Creek its arrival at 1135 EST was accompanied by a pressure jump on the order of 2 mb and a small temperature fall of 2°C (from 32°C); see Fig. 17. These were preceded by a gradual change in wind direction from a westerly before 1000 EST through a northerly just before 1100 EST to a southerly at the time of the change. There was no apparent surface signature at Richmond (Fig. 18) and only a weak signature at Hughenden at around 2020 EST (data not shown). There, the wind freshened and the surface temperature began to rise steadily, presumably as the surface-based evening radiation inversion was removed. Subsequently, over a period of about 40 min, the wind backed progressively to a south-southwesterly and at 2100 EST the temperature began to fall steadily at a rate of

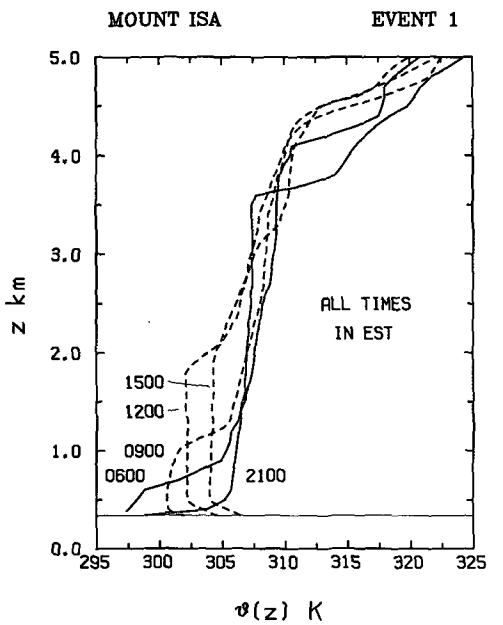

FIG. 14. Vertical profiles of potential temperature $\theta_v(z)$ in the prefrontal and postfrontal air masses at Mount Isa for the first event during CAFE, which arrived at Mount Isa at 0940 EST 10 September. The soundings at 2100 EST 9 September and at 0600 and 0900 EST 10 September are therefore about 13, 3, and 1 h before the frontal passage, respectively. The soundings at 1200 and 1500 EST are about 2 and 5 h after the frontal passage.

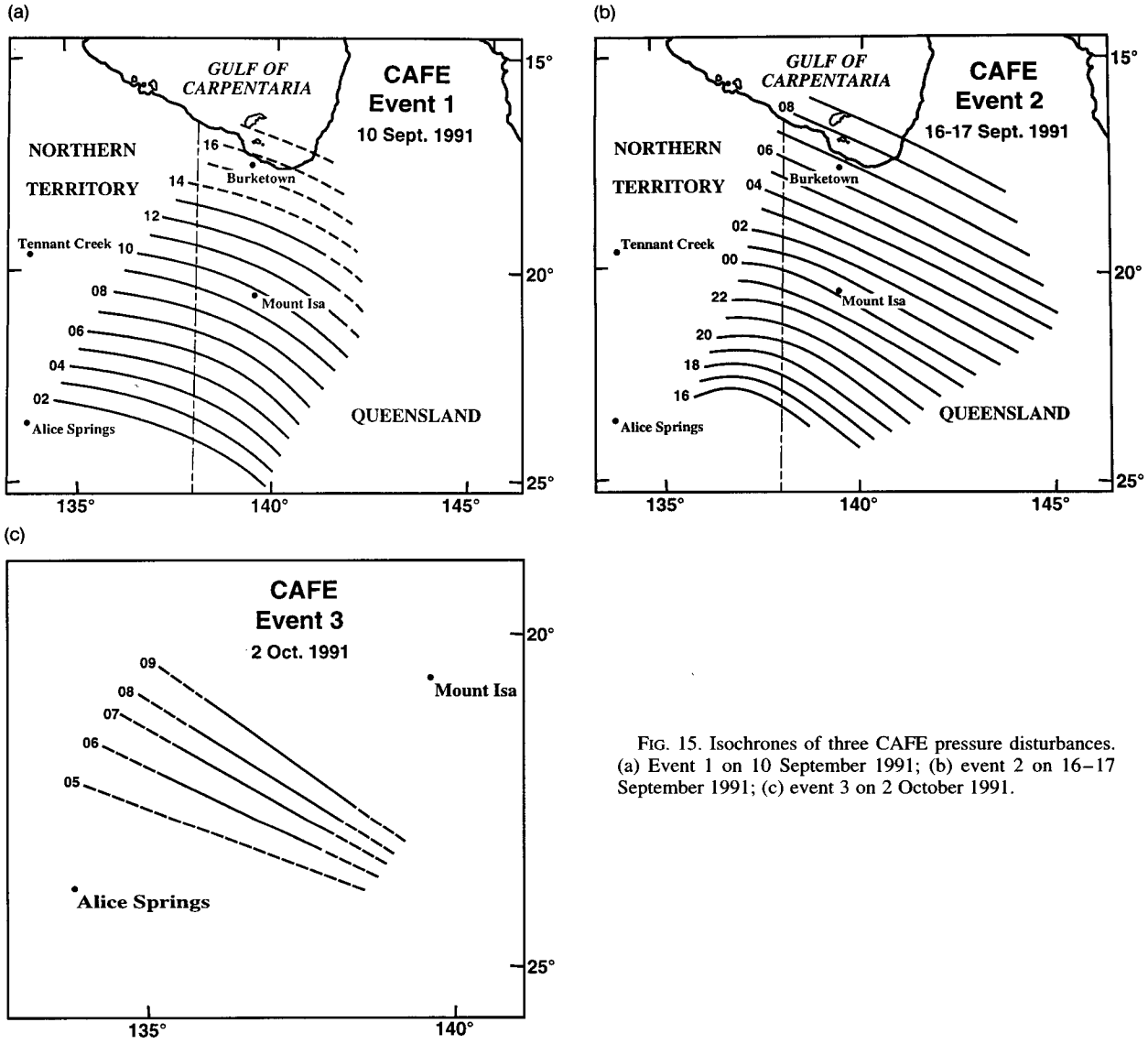

FIG. 15. Isochrones of three CAFE pressure disturbances. (a) Event 1 on 10 September 1991; (b) event 2 on 16–17 September 1991; (c) event 3 on 2 October 1991.

2.5°C h^{-1}. The backing of the wind, predominantly between 2000 and 2100 EST, is evident in the low-level wind field obtained from the hourly pilot balloon soundings at Hughenden (Fig. 19) and the cooling accompanying the disturbance aloft is confirmed by the prefrontal and postfrontal soundings there at 1800 and 2200 EST (Fig. 20). In addition to the average cooling of about 5°C in the lowest 1 km, there was a marginal reduction (on the order of 1 g kg^{-1}) of moisture in this layer.

b. Event 2

Although a significant disturbance throughout most of our observational network, this front produced no clear surface signature at Alice Springs and Harts Range where backward extrapolation of the isochrones in Fig. 15b suggests that it should have passed during the afternoon. The Bureau of Meteorology objective analyses showed that the front, as defined by the wet-bulb potential temperature gradient, had stalled over the Alice Springs region during the daytime. The radiosonde sounding at Alice Springs at 1500 EST on that afternoon showed slight cooling (maximum 3°C) below 2 km compared with the sounding 6 h earlier with a mixed layer extending only 1.5 km AGL.[2] Since a temperature rise would normally be expected during this time period, we may surmise that the airmass change had taken place at Alice Springs by 1500 EST as suggested by the isochrones.

[2] There was also a slight increase (~1 g kg^{-1}) of moisture in this layer.

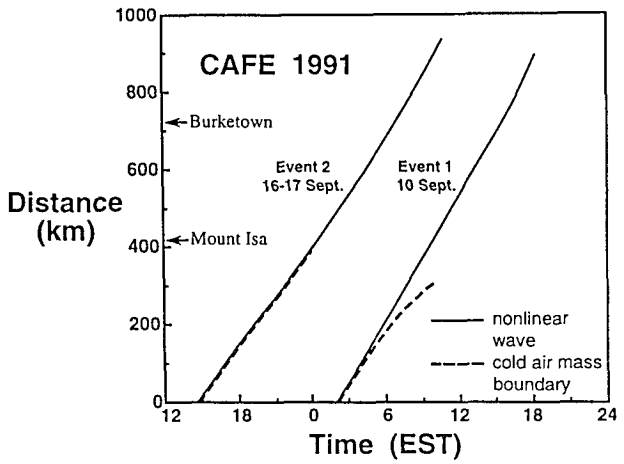

FIG. 16. Position of the leading edge of the pressure disturbance and the cold air mass boundary at the surface along a line through Burketown, and oriented approximately normal to the disturbance for the first and second CAFE events.

At other stations in the southwestern part of the network, the frontal passage was marked by an abrupt pressure jump, a sharp increase in wind, a rapid change in wind direction, and a sharp decline in temperature *and* mixing ratio. At Boulia the frontal passage was dramatic with the surface wind speed reaching nearly 12 m s^{-1} as the wind turned to the south and the pressure rose 3 mb in 20 min (Fig. 21). The temperature fell 8°C in this period. Sudden large temperature decreases of 4°C were recorded at Marion Downs and

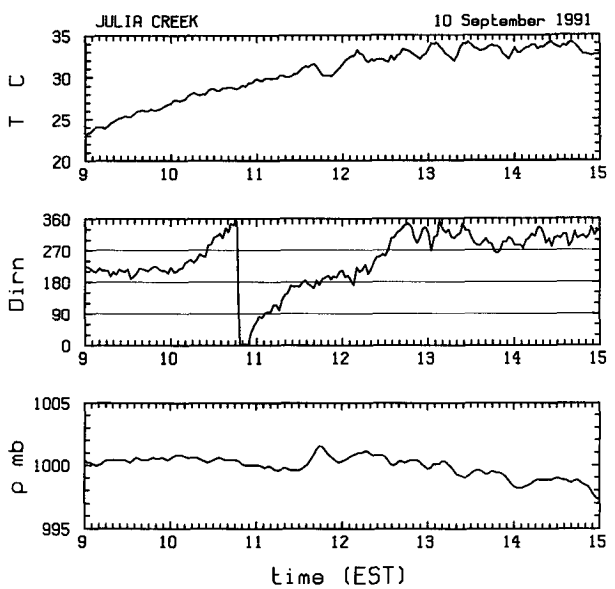

FIG. 17. Surface station data at Julia Creek surrounding the passage there of the first event during CAFE. (a) Temperature; (b) wind direction; and (c) pressure (wind speed and humidity data were unavailable).

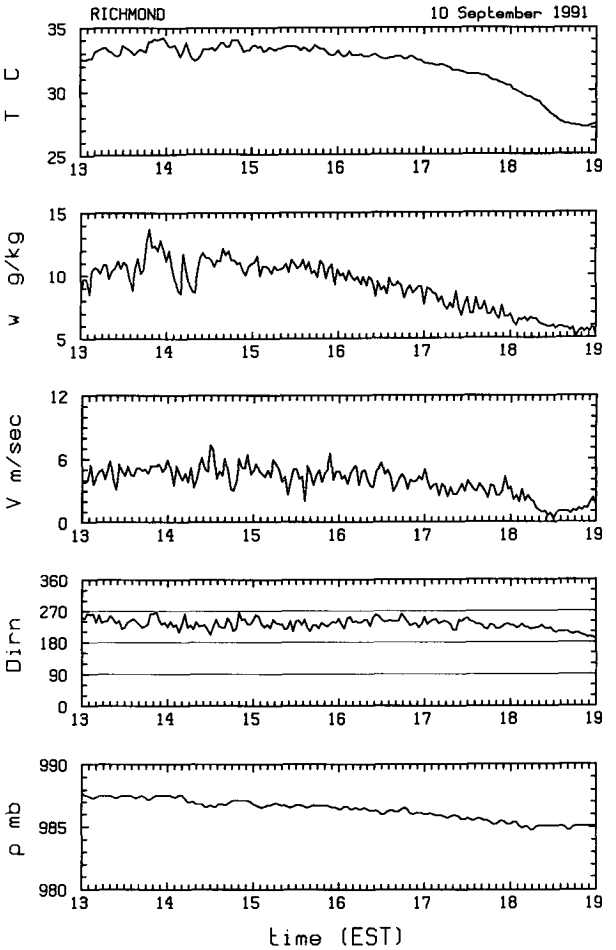

FIG. 18. Legend as for Fig. 6 except for Richmond.

Dajarra, and the total temperature decrease at Marion Downs over a period of 2 h was about 7°C, comparable with that at Boulia. Elsewhere in this region, the pressure jump was more modest, between 1 and 2 mb. The front passed Urandangi at 2050 EST at which point it still had the character of a single change. In contrast to CE1, the airmass boundary was accompanied by a temperature fall at every station.

Figure 22 shows the evolution of the pressure signature at stations north of 20°S for this event. At Camooweal at about 0035 EST 17 September, the pressure signature showed predominantly a single jump, but by the time the disturbance had reached Thorntonia Station around 0230 EST it had already developed a pressure signature characteristic of an undular bore in which form it reached the southern coast of the Gulf of Carpentaria around 0700 EST. The early development of a double changelike structure is evident in the low-level wind structure at Mount Isa obtained from the wind profiler there and shown in Fig. 23. There was an initial change below about 700 m AGL at 0030 EST, but this was followed at 0040 EST by a return to es-

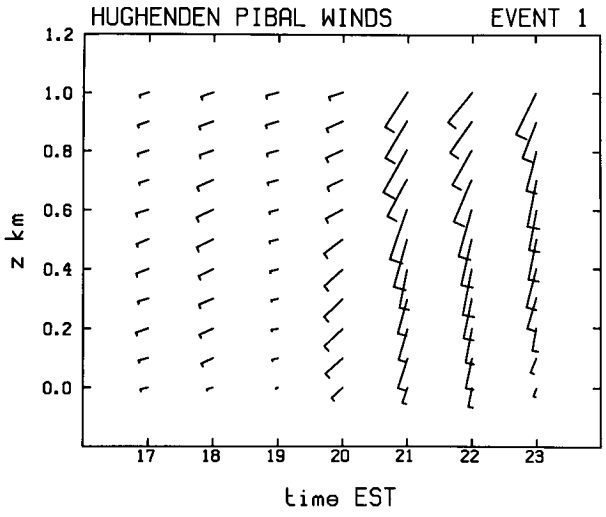

FIG. 19. Time–height display of the horizontal low-level wind vectors obtained from hourly pilot balloons released at Hughenden during the first CAFE event. Note particularly the backing between 2000 and 2100 EST. Wind vectors are scaled so that 1 h along the abscissa corresponds with a wind speed of 20 m s^{-1}.

sentially prefrontal conditions. The second change occurred some 5–10 min later. There was no evidence for a sudden temperature decrease at Lake Nash, but the event was marked there by a sudden change in the rate of cooling from 0.9°C h^{-1} to 2.3°C h^{-1}. Moreover, there was no obvious indication of an airmass change

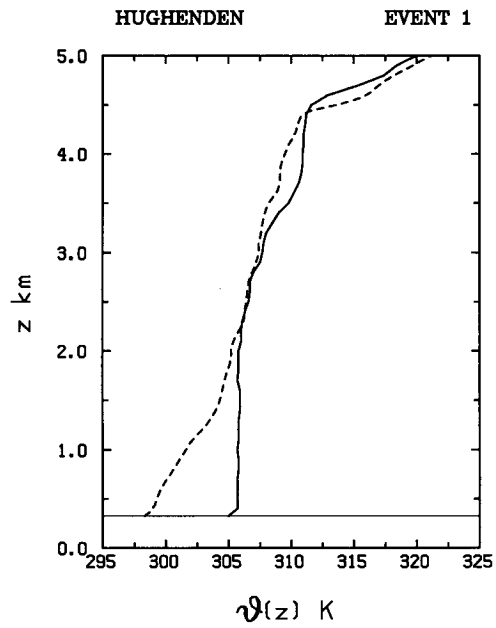

FIG. 20. Vertical profiles of potential temperature $\theta(z)$ in the prefrontal and postfrontal air masses at Hughenden for the first CAFE event. The solid and dashed lines are the 1800 and 2100 EST soundings, respectively.

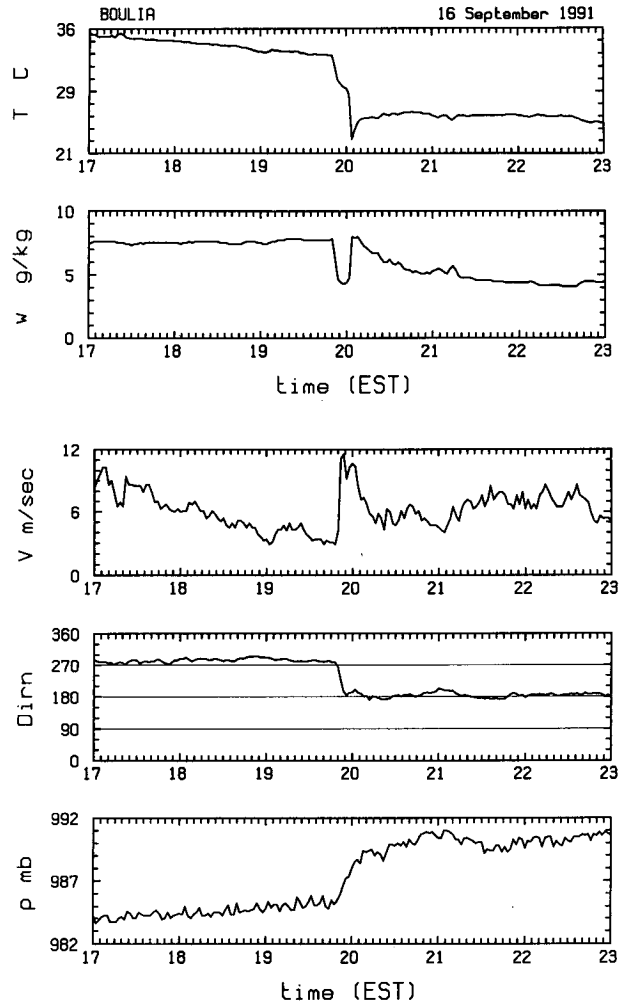

FIG. 21. Legend as for Fig. 6 except for Boulia during the second CAFE front.

in the surface temperature records from Camooweal and other sites farther north (Fig. 16).

To the southwest of Mount Isa, the average speed of the pressure disturbance was 12.0 ± 0.2 m s^{-1} from 205°. The observations suggest that the disturbance slowed down slightly, to about 11.4 ± 0.2 m s^{-1} over the area immediately to the north of Mount Isa, probably due to the higher topography, and then speeded up as the waves became well developed. In the gulf region and over the southern part of Cape York Peninsula the speed had increased to 15.6 ± 0.2 m s^{-1}. It is possible that this acceleration can be attributed in part to the movement of the disturbance into a deeper and stronger stable layer as provided by the inland intrusion of sea-breeze air from the gulf on the previous day. While we do not have data to determine the inland extent of this intrusion on 16 September, we can say that conditions were favorable for this with a strong northerly sea breeze at Burketown during the afternoon un-

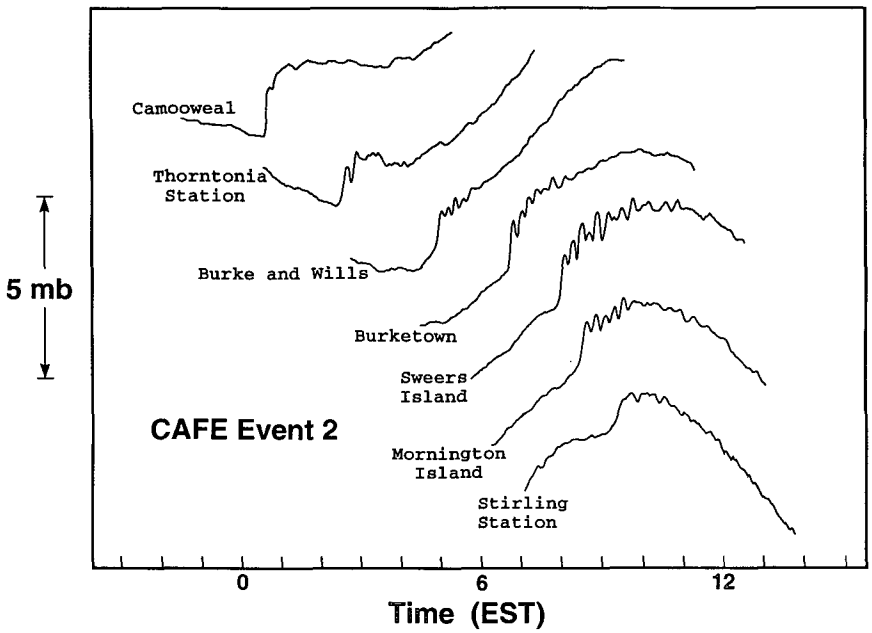

FIG. 22. Surface pressure signatures recorded at microbarograph stations at and to the northeast of Camooweal during the second CAFE event. As in Fig. 11, the signatures are arranged sequentially. Again, note the development of an undular borelike signature as the disturbance moves northeastward during the night and early morning.

der conditions of a northeasterly geostrophic flow (see, e.g., Physick and Smith 1985). Another factor in the acceleration is the typical increase in wave speed that occurs when nonlinear waves increase in amplitude during the normal evolution process (Whitham 1974). Finally, the slight downhill slope of the topography to toward the coast may have played a role also.

As they approached moister air near the gulf coast, the bore waves generated a pair of spectacular "morning glory" roll clouds. These are seen in satellite imagery to be over 300 km long, aligned along the pressure disturbance (cf. Fig. 15b), and separated by a distance of about 20 km (Fig. 24).

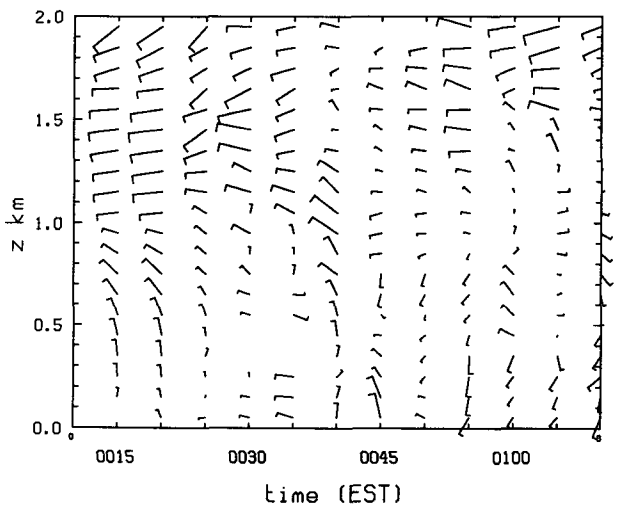

FIG. 23. Time–height display of horizontal wind vectors based on data obtained from the Mount Isa wind profiler during the passage of the second CAFE event. The first low-level wind change occurs at about 0030 EST, but is short lived with a return to northerlies at 0040 EST. The second change occurs at 0050 EST. As in Fig. 12, the wind vectors are scaled so that 5 min along the abscissa corresponds with a wind speed of 20 m s^{-1}.

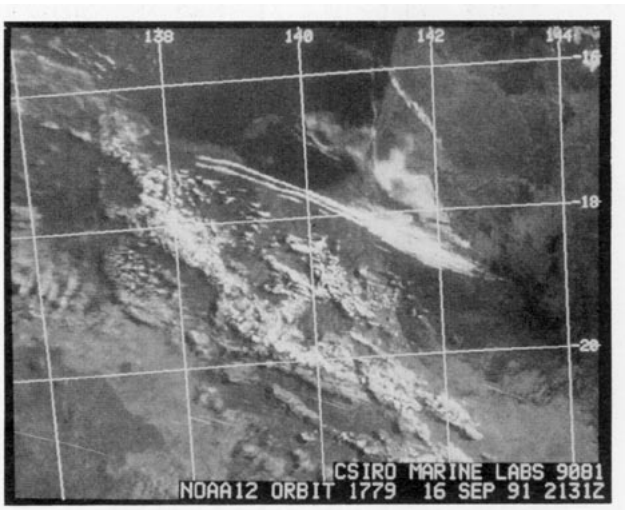

FIG. 24. *NOAA-12* AVHRR visible satellite image at 0730 EST 17 September 1991.

Positive identification of the borelike structure in the gulf region was provided by a pair of radiosonde soundings at Burketown, one at 0430 EST, approximately 2 h before the passage and the other at 0922 EST, some 3 h after the passage of the leading cloud roll. Figure 25 shows the vertical profiles of potential temperature θ, and mixing ratio w, obtained from these soundings. A characteristic of a bore is that the relative streamlines, and therefore air parcels, are permanently displaced in the vertical following its passage. This behavior is exemplified by the streamlines for the morning glories of 11 and 20 October 1981 documented by Smith and Morton (1984, see their Figs. 9, 10, and 18). A consequence is that air with lower potential temperature is permanently lifted in the layer affected by the bore, but not of course at the surface where the vertical velocity is zero. The result is cooling aloft when one compares the pre- and postdisturbance soundings. In

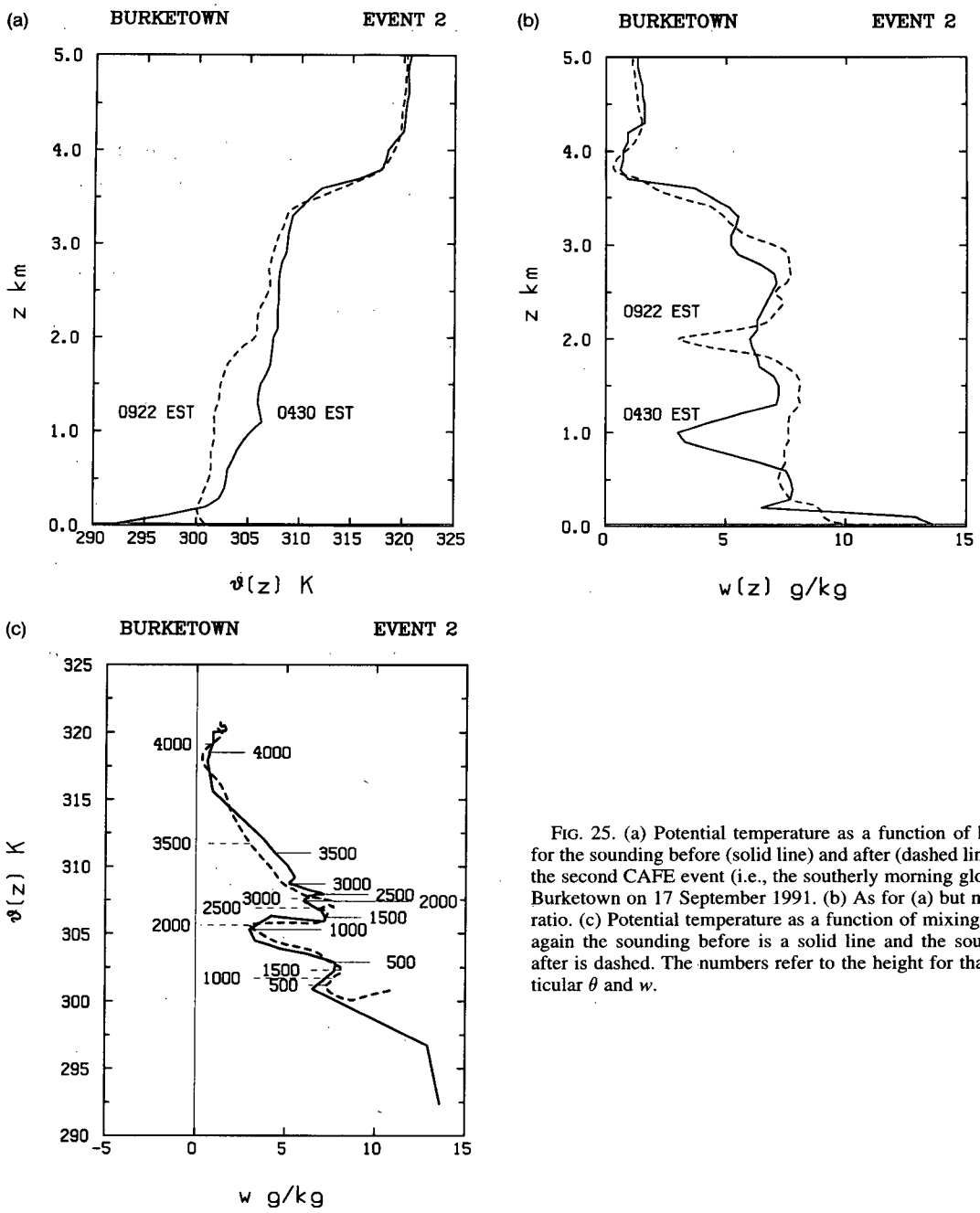

FIG. 25. (a) Potential temperature as a function of height for the sounding before (solid line) and after (dashed line) for the second CAFE event (i.e., the southerly morning glory) at Burketown on 17 September 1991. (b) As for (a) but mixing ratio. (c) Potential temperature as a function of mixing ratio; again the sounding before is a solid line and the sounding after is dashed. The numbers refer to the height for that particular θ and w.

contrast, an airmass change brought about by the horizontal advection of cooler air would normally bring about cooling at the surface as well. It follows that, in theory, one should be able to distinguish between a bore and a more conventional cold front or gravity current by examining the change in the potential temperature of the air at the surface. In practice, however, as we have seen, both types of disturbance may bring about an *increase* in surface air temperature by destroying any surface-based radiation inversion through surface mixing. An alternative method of distinguishing a bore from a gravity current is to use a second conserved tracer such as the mixing ratio or the equivalent potential temperature θ_e, a method that has been used also by Koch et al. (1991; see their Fig. 19). Inspection of Fig. 25b shows a dry layer in the predisturbance mixing ratio trace and it would appear that this layer is lifted about 1 km following the passage of the disturbance. On the assumption that θ and w are conserved along streamlines, the profile of θ versus w should be the same before and after the passage, although the height corresponding with a particular θ and w will have changed. Figure 25c shows the pre- and postdisturbance $\theta(w)$ profiles based on the foregoing soundings and indicates the height $z(\theta)$ at 500-m intervals for each profile. It will be seen that at heights above 500 m there is close agreement between the two curves confirming the borelike structure of the disturbance. A change in air mass brought about by horizontal advection would not be expected to produce such agreement. However, below 500 m convective mixing had already begun to alter the postdisturbance distributions of $\theta(z)$ and $w(z)$, destroying the predisturbance $\theta(w)$ relationship there.

c. *Event 3*

The front passed through Alice Springs at 0200 EST 2 October. It was marked there by a sharp change in wind direction from a north-northwesterly to a south-southwesterly, an abrupt rise in dewpoint temperature (from −10°C to 2°C in 10 min) and a 1-mb pressure jump. The surface wind speed increased from about 5 m s^{-1} before the passage to about 8 m s^{-1} after the passage and the temperature declined steadily. The leading disturbance in this frontal system was recorded at the CAFE surface stations closest to Alice Springs in the form of a series of solitary wave components moving northeastward at a speed of about 10 m s^{-1} (the isochrones are shown in Fig. 15c). The upper-air sounding there at 0300 EST showed a moderate (~10 m s^{-1}) southerly flow in the lowest kilometer AGL in contrast to the light northeasterly that was present at 2100 EST 1 October. There was a marked cooling (~10°C) also in this layer (Fig. 26) between the radiosonde soundings at 1900 EST 1 October and 0300 EST 2 October indicative of an airmass change. Figure 27 shows the surface wind and pressure data at Tarlton Downs and Argadargada for this event where the wavelike structure is most apparent, but there was no evidence that it was accompanied at these stations by an airmass change. At Harts Range there was a slight rise in pressure, but no more than 0.5 mb about 0500 EST; otherwise there was no obvious surface signature of an airmass change. In contrast, at Jervois there was a single, sharp pressure jump of about 2.1 mb at 0525 EST accompanied by a well-defined temperature jump that merged into the normal pattern of temperature increase after sunrise. It is possible that the airmass boundary coincided with the pressure jump, but there is no firm evidence for this. At Tobermory Station the disturbance was recorded as a weak group of solitary waves with onset around 0916 EST. Their maximum pressure amplitude was about 0.8 mb and they were accompanied by a small increase in temperature (on the order of 0.8°C) and short lived (about 20 min) drop in pressure. Presumably, by this stage the disturbance was being rapidly destroyed by the reestablishment of deep convective mixing in the boundary layer. It was not detectable at any of the other stations in the network, even at Marion Downs and Boulia. The other nearby station, Urandangi, was not operating on this day. The available data for this event are too sparse to allow any real conclusions, except that it appears that solitary waves had effectively separated from the airmass boundary by the time they reached Tarlton Downs and Argadargada.

d. *Synthesis*

All fronts showed a marked diurnal variation in the subtropics, being difficult to locate during the late morning and afternoon, but developing a sharp surface change after sunset. Such development appeared to be associated with rapid nocturnal frontogenesis in the semipermanent low-latitude trough, which can be attributed in part to the heating of the continent. The cold airmass boundary in CE1 decelerated markedly during the daytime, whereas CE2 had crossed the network by 1000 EST and CE3 did not survive beyond that time. All three fronts excited large-amplitude wave motions in the early morning, which propagated ahead of the airmass change by distances of over 40 km on a surface-based nocturnal radiation inversion. Thus the frontal system appeared for periods of up to about 12 h to have the form of a double change, the leading change being manifest at the surface by an abrupt wind surge (or a series of wavelike surges) and accompanied by a pressure jump and frequently a temperature rise.[3] The second change marks the passage of the airmass boundary and brings a temperature fall and a change in the

[3] We note that the flow may still be hydrostatic since the temperature rise occurs in a very shallow layer. The cold air (which is potentially warmer than that in the shallow inversion layer) is much deeper.

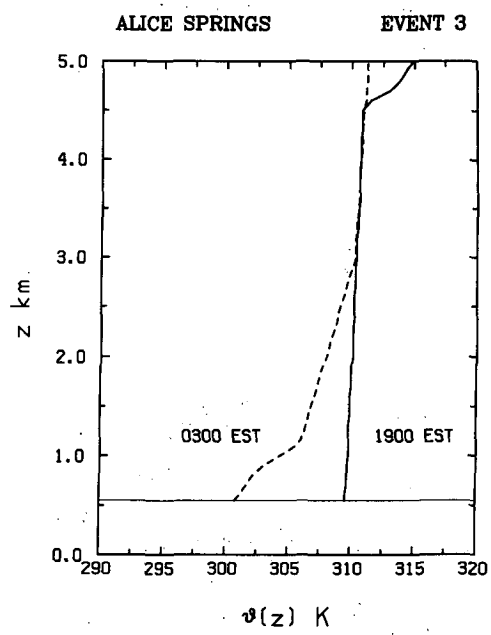

FIG. 26. Vertical profiles of potential temperature $\theta(z)$ in the prefrontal and postfrontal air mass at Alice Springs for the third event during CAFE.

moisture content of the air. This behavior is exemplified well by the surface data for CE1 at Argadargada (Fig. 8) and Urandangi (Fig. 9). The nonlinear wave becomes progressively modified as the convective mixing recommences, but in both CE1 and CE2 it remained a significant feature until 0900–1000 EST.

Observations of wavelike structures at Mount Isa and nearby stations until 1000 EST during CE1, along with upper-air soundings at Mount Isa (Fig. 14), suggest that in the hours after sunrise the nonlinear wave disturbance in this case must have continued to propagate on the elevated inversion at the top of the newly developing well-mixed layer since the surface-based stable layer there had already been removed by the time the front arrived.

Dynamical aspects of the apparent daytime weakening of cold fronts over central Australia and possible mechanisms for their reformation after sunset are discussed in section 6.

5. Surface energetics

It is clear that the nature and behavior of continental cold fronts in the Australian subtropics is strongly modulated by the surface energy transfer. To provide data on this a detailed set of observations of shortwave irradiance (total, diffuse, and reflected), longwave irradiance (atmospheric and terrestrial), and surface heat fluxes (sensible, evaporative, and substrate) was obtained over natural grassland at Hughenden Aerodrome.

The typical diurnal variation of the surface energy balance at Hughenden throughout the period is well represented in the plot for 16–17 September (Fig. 28). CE2 passed through Hughenden at about 0600 EST 17 September. Apart from some slight cloud effects on that afternoon, net all-wave irradiance Q^* was similar on both days, peaking at 500 W m^{-2} around noon, with a nocturnal radiative deficit averaging approximately -70 W m^{-2}. On 16 September approximately 60% of net irradiance was partitioned into sensible heating of the atmosphere (Q_H), with much of the remainder being utilized in heating of the soil substrate (Q_G), while

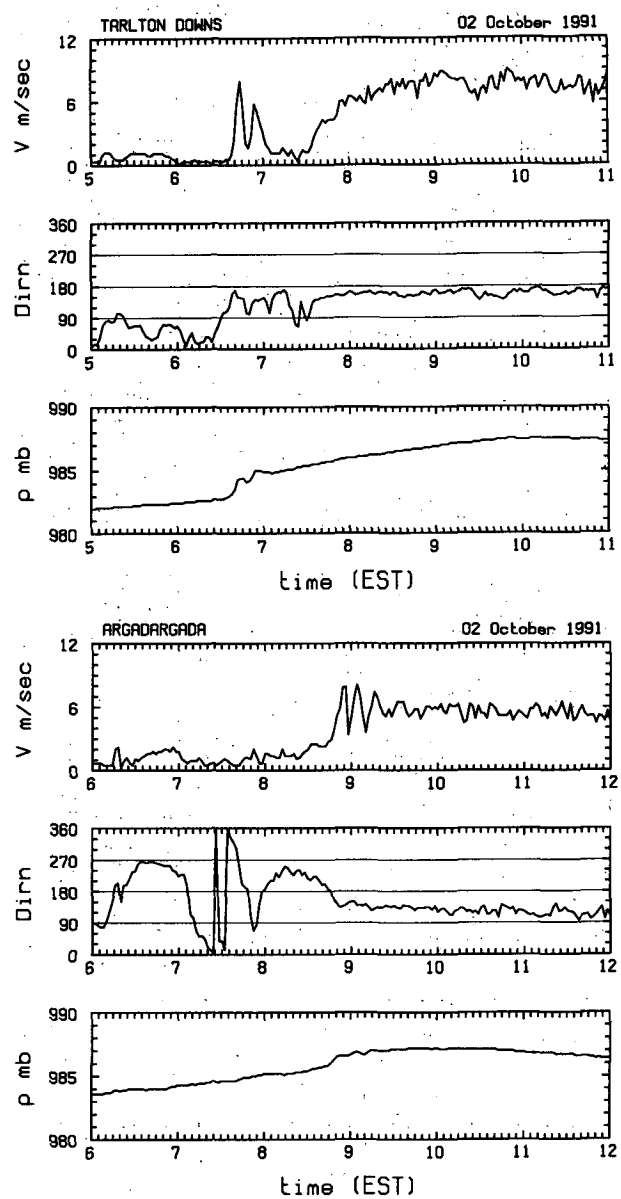

FIG. 27. Surface variation of wind speed, wind direction, and pressure at Tarlton Downs and Argadagada during the passage of the third CAFE front on 2 October 1991.

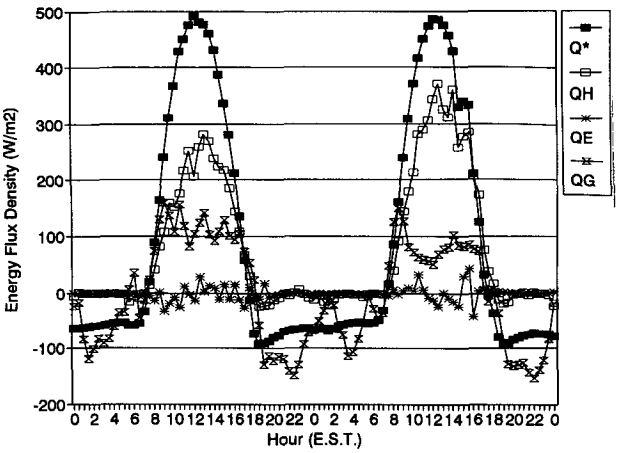

FIG. 28. Surface energy balance measured at Hughenden on 16–17 September 1991. Here Q^* is the net all-wave irradiance; Q_H and Q_E are the sensible and evaporative heat fluxes, respectively; and Q_G is the substrate heat flux. The second CAFE front arrived at Hughenden at about 0600 EST 17 September 1991.

on the following day as much as 75% of net irradiance was partitioned into sensible heat flux. The greater sensible heat flux on this day would appear related to the advection of a much cooler air mass, resulting in an enhanced thermal gradient between the surface and lower atmosphere. Evaporative heat flux Q_E was negligible on both days. The nocturnal radiative deficit on each day is primarily balanced by a transfer of heat from the substrate, but this flux was strongly affected by environmental factors at the surface (note the nocturnal fluctuation in Q_G associated with the turbulent mixing down of warm air to the surface during periods of stronger winds).

6. Dynamical considerations

Analysis of the three events sampled during CAFE has demonstrated that cold fronts do penetrate into the subtropics, and that these fronts may, in turn, generate bore waves or solitary wave trains that propagate still further equatorward. Such observations raise fundamental questions concerning the dynamics of subtropical cold fronts. For example:

(i) Why do low-latitude fronts show such little surface signature during the daytime while rapidly intensifying after sunset?

(ii) What is the precise generation mechanism for the nonlinear waves that were observed?

While definitive answers to these questions await further research, we offer now a largely speculative explanation.

Individually, the dynamics of dry buoyant boundary layer convection and the dynamics of inviscid adiabatic midlatitude frontogenesis are, for the most part, well understood. In contrast, there has been very little attention paid to the effect of the convective boundary layer on frontal development, a problem central to understanding the behavior of subtropical cold fronts over the Australian interior. Some insight is provided by simplified midlatitude numerical model calculations by Reeder (1986) and Reeder et al. (1991). These investigations, together with a recent study of frontogenesis in the presence of convective mixing in the context of sea-breeze fronts by Reible et al. (1993), are pertinent to the discussion that follows.

Figure 29 shows time–height cross sections of potential temperature at Mount Isa for CE1 and CE2. Although it is not valid to invoke a time-to-space conversion in the presence of the large diurnal changes, it is clear that, despite the deep convective mixing of the warm air mass and the strong heating of the cold air mass during the day, there remains a significant temperature contrast between the prefrontal and postfrontal air (see also Figs. 2 and 3). It is evident also that in the cold air mass the heating is opposed locally by cold-air advection and that the latter continues after the heating has ceased.

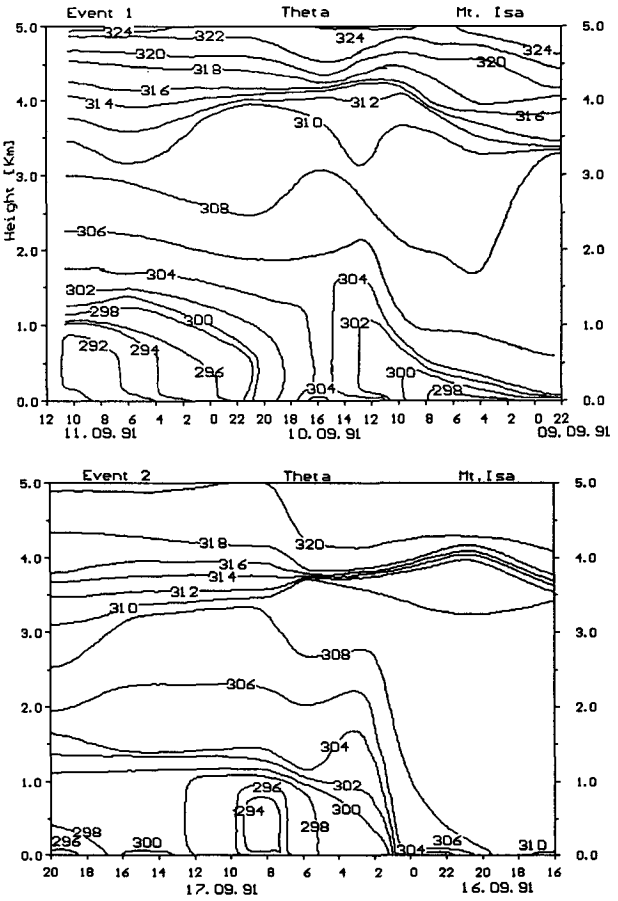

FIG. 29. Time–height cross sections of potential temperature at Mount Isa for (a) CAFE event 1 and (b) CAFE event 2.

To put matters into focus, we consider frontogenesis in a two-dimensional model. Let (x, y, z) be a rectangular coordinate system with x directed normal to the surface front toward the warm air, y along the front, and z pointing vertically upward. Let (u, v, w) denote the corresponding velocity components in these directions. Then the frontogenesis equation (Miller 1947) takes the form

$$\frac{D}{Dt}\left[\frac{\partial\theta}{\partial x}\right] = -\frac{\partial u}{\partial x}\frac{\partial\theta}{\partial x} - \frac{\partial v}{\partial x}\frac{\partial\theta}{\partial y} - \frac{\partial w}{\partial x}\frac{\partial\theta}{\partial z} + \frac{\partial}{\partial x}(\nabla\cdot\mathbf{q}), \quad (1)$$

where θ is the potential temperature, $\mathbf{q}$ is the eddy heat flux, and D/Dt denotes the usual material rate of change.

Across central Australia during the daytime it is reasonable to assume that $\mathbf{q}$ is dominated by the vertical heat transport associated with dry convection. Furthermore, it is clear from Figs. 14 and 29 that both the cold and warm air masses are vertically well mixed at such times. It is therefore appropriate to consider the vertically integrated effect on frontogenesis or frontolysis of the term in (1) involving $\mathbf{q}$. Suppose that an hour or two after sunrise, the nocturnal radiation inversion has been removed from both air masses as suggested by Figs. 14 and 29. Then, assuming a simple zero-order closure model for the mixed layer (see, e.g., Garratt 1992, chapter 6; Carson 1973), it follows that the mixed-layer potential temperature θ_m increases with time according to

$$\theta_m = [\Gamma^2 h_0^2 + 2\Gamma(1+\beta)Q_H t]^{1/2} - \Gamma h_0, \quad (2)$$

where h is the mixed-layer depth, h_0 is the mixed-layer height shortly after sunrise, Γ is the static stability of the air above the mixed layer, and β is the ratio of the turbulent heat flux by entrainment through the top of the mixed layer to Q_H, normally assumed constant (Garratt 1992). The energy balance observations discussed in the previous section indicate that Q_H is slightly greater in the cold air mass than in the warm air mass. Further, Figs. 14 and 29 suggest that Γ is greater in the cold air, but h_0 is greater in the warm air mass than in the cold air mass. Thus, the observed variations in the parameters Q_H, Γ, and h_0 with the front's passage imply that, insofar as Q_m is governed by (2), Q_m will increase more rapidly on the cold side of the airmass change than on the warm side. It follows that, on the frontal scale, the gross effect of dry convective heating represented by the last term in (1) is likely to be frontolytic, although larger-scale spatial variations in surface sensible heat flux may be expected to maintain the broadscale temperature gradient.

Possible frontogenesis processes are represented by the first three terms on the right-hand side of (1). These may be associated with the action of synoptic-scale patterns of deformation together and the cross-frontal circulation in the x–z plane on preexisting temperature gradients (Hoskins and Bretherton 1972). It is possible that the necessary background temperature gradients may be provided by differential sensible heating. Although direct measurements do not exist, one expects the sensible heat flux to vary substantially on the synoptic scale due to large-scale inhomogeneities in the albedo and Bowen ratios, and the dependence of the irradiance on latitude. Indeed, the heat troughs of northern Australia are thought to be a result of a combination of orographic effects and horizontal gradients in sensible heating. [Aspects of the dynamics of the Australian heat troughs may be found in Fandry and Leslie (1984), Adams (1990), and Kepert and Smith (1992).] Figures 2b, 3b, and 4b show prominent low-level potential temperature maxima associated with heat troughs, and it is reasonable to presume that these maxima result, at least partially, from differential heating. Of relevance to the present discussion is the northwest–southeast-oriented band of pronounced temperature gradient on the southwestern side of the heat trough. Thus, the deformation provided by the wind field associated with the approaching front may act to enhance such temperature gradients.

In the case of sea breezes, the background temperature gradient is provided by differential sensible heating across the coastline, and the cross-frontal circulation is gravity driven. In this case frontogenesis is associated principally with the term $-(\partial u/\partial x)(\partial\theta/\partial x)$ in (1) as discussed by Rieble et al. (1993). The latter authors argue that the development of a sharp sea-breeze front depends inter alia on the relative magnitude of this term compared with the frontolytic effect of the dry convective heating. In particular they present observations that suggest that the development of a sharp sea-breeze front in the late afternoon may be attributed to the decline in the strength of the convection, allowing frontogenesis to proceed relatively unhindered.

It seems reasonable to interpret the diurnal variation of the strength of cold fronts over central Australia in similar terms, although the processes responsible for frontogenesis may be different. It is still unclear to what extent gravitational effects contribute to the cross-frontal circulation, but it is known that the local structure of CE1 and CE2 at Mount Isa was *unlike* that of the classical laboratory gravity current. There, the frontal speed c was significantly in excess of the low-level wind speed in the direction of motion of the front so that there was no low-level feeder flow of cold air toward the front. In other words, the pressure jump line was not moving as a material surface (cf. Smith and Reeder 1988). Wind profiler data at Mount Isa showed that in both CE1 and CE2, values of $u - c$ were negative up to at least 2 km above ground in the first hour after the passage of the leading disturbance, the maximum values being around -3.0 m s^{-1}. This is consis-

tent with the fact that the leading edge of both disturbances had a wavelike structure at Mount Isa. Unfortunately, in neither case could we determine the speed of the airmass boundary in the neighborhood of Mount Isa, although at least in CE2, where the wavelike structure was in its early stages of evolution, this speed is unlikely to differ much from that of the leading change. At Boulia in CE2, the surface values of $u - c$ reached values greater than -1.0 m s^{-1} for about 10 min immediately following the frontal passage, suggesting that there might have been a region aloft where $u - c$ attained positive values during this time. There was only a single change there, so that the disturbance speed and the speed of the airmass boundary were the same. Even so, the relatively short duration of this (possible) pulse of relative flow toward the front suggests that classical gravity current dynamics is unlikely to apply near the front. The arguments presented above suggest that the effect of dry homogeneous convective heating is probably frontolytic, in agreement with the observed behavior of frontal systems over central Australia. However, horizontal inhomogeneities in sensible heating may help provide the background temperature gradient needed for frontogenesis. At night, after the turbulent mixing has effectively ceased, frontogenesis proceeds unhindered. Nevertheless, the theoretical understanding of this problem is clearly more complicated than these arguments alone imply.

During the night, with the cessation of sensible heating, the turbulent boundary layer stress is greatly reduced and a shallow nocturnal inversion quickly develops below the deep well-mixed layer formed during the day. In response to the sharply reduced stress, air parcels in the remnant mixed layer accelerate, a component of the acceleration pointing down the pressure gradient. We hypothesize that it is the large parcel accelerations and subsequent convergence into the trough associated with this sort of adjustment that generate the kind of solitary wave train observed in all the CAFE events. Similar phenomena are known to occur when a gravity current moves into a surface-based stably stratified layer as mentioned earlier. While it is not possible to determine the extent to which the front can be regarded locally as a gravity current (cf. Smith and Reeder 1988, section 3), the mechanism of solitary wave formation may not depend crucially on the precise details of the forcing (see, e.g., Christie 1989). Further observational and theoretical work on the detailed mechanisms that govern the evolution of subtropical continental cold frontal systems is clearly called for.

7. Summary and conclusions

Data gathered during two recent field experiments in central and northern Australia have enabled us to document in unprecedented detail the structure and evolution of cold fronts that are a common feature in the Australian subtropics during the dry season (approximately May–October). Typically, such fronts are often dry, are shallow (~1 km deep), and move into a deep convectively well-mixed boundary layer which, during the night, overlies a strong but shallow radiation inversion.

The synoptic environment of these fronts is similar to that of the summertime "cool change" of southeastern Australia[4] with frontogenesis occuring in the col region between the two subtropical anticyclones, relatively far from the center of the parent cyclone. A unique feature of the region is the presence of heat troughs over northeastern Western Australia and northwestern Queensland with which the frontal trough eventually merges. Generally, the frontal passage is followed by strong ridging from the west.

The data obtained during the CAFE experiment highlight the large diurnal variation of frontal structure associated with diabatic processes. The fronts are often difficult to locate during the late morning and afternoon when convective mixing is at its peak, but develop strong surface signatures in the evening as the convection subsides and a surface-based radiation inversion develops. Moreover, there appears to be a ubiquitous tendency in the early morning for the formation of a nonlinear wavelike or borelike structure at the leading edge of the frontal zone as the inversion strengthens. In each case, as the wave/bore developed, it was observed to propagate ahead of the airmass change on the preexisting inversion. Such behavior was exemplified by the data for CE1 and CE2. In the latter case, the data are unique in providing the first clear evidence of the formation of a southerly morning glory bore wave in the Gulf of Carpentaria region from a cold front in the south. The passage of the bore brings a strong but temporary wind surge at the surface accompanied by a sharp pressure jump. These are followed by a series of wind and pressure oscillations with a period of 10–15 min, before the steadier postfrontal airflow is established. Our observations are consistent with the idea that the penetration of a disturbance into the southern gulf region in the form of a southerly morning glory is favored by an evening passage of the front through Mount Isa. In this case, the disturbance is not subject to the destructive effect of strong diabatic heating on its way to the gulf.

Modeling studies are being carried out at present to investigate the frontolysis and deceleration of fronts during the daytime and their reintensification and acceleration during the evening, as well as their generation of nonlinear wave- or borelike disturbances.

Acknowledgments. We would like to record our gratitude to the Bureau of Meteorology for its support,

[4] A recent review of the summertime "cool change" is given by Reeder and Smith (1992).

fice in Melbourne, to the Queensland and Northern Territory Regional Offices, and to the Weather Offices in Mount Isa, Alice Springs, and Townsville. Thanks are due to Mt. Isa Mines for providing the profiler data, to CSIRO Division of Atmospheric Research for the satellite picture, and to Qantas Airlines for their assistance with the transportation of equipment from Germany. We are indebted also to the following field participants from Monash University, the University of Munich, and the Australian National University: Norbert Beier, David Brown, Karin Bückner, Klaus Dengler, John Grant, Morwenna Griffiths, Ritschie Heinrich, Annette Hellmeier, Noreen Krusel, Heinz Lösslein, Anita Menhofer, David Packham (who piloted the light aircraft), and Allyson Williams. Thanks go also to Konrad Häckl of the University of Munich for much behind-the-scene organizational assistance and Hilbert Wendt at the University of Munich and Phil Scamp of Monash University, who each drafted several of the figures. Lee Andrews and Sheryl Lucas of Monash University, and Anna-Riitta Järvinen of the University of Munich all contributed to typing the manuscript. Financial support for CAFE was provided by the Australian Research Council, the German Research Council, and the Bureau of Meteorology Severe Weather Program Office.

Finally, we are indebted to Dr. Fred Sanders and two anonymous reviewers for their very detailed and constructive comments on the original version of the manuscript.

REFERENCES

Adams, M., 1986: A theoretical study of the inland trough of northeastern Australia. *Aust. Meteor. Mag.*, **34,** 85–92.

Carson, D. J., 1973: The development of a dry inversion-capped convectively unstable boundary layer. *Quart. J. Roy. Meteor. Soc.*, **99,** 450–467.

Christie, D. R., 1989: Long nonlinear waves in the lower atmosphere. *J. Atmos. Sci.*, **46,** 1462–1491.

——, 1992: The morning glory of the Gulf of Carpenteria: A paradigm for nonlinear waves in the lower atmosphere. *Aust. Meteor. Mag.*, **41,** 21–60.

——, K. J. Muirhead, and R. H. Clarke, 1981: Solitary waves in the lower atmosphere. *Nature*, **293,** 46–49.

Clarke, R. H., 1972: The morning glory: An atmospheric hydraulic jump. *J. Appl. Meteor.*, **11,** 304–311.

——, R. K. Smith, and D. G. Reid, 1981: The morning glory of the Gulf of Carpentaria: An atmospheric undular bore. *Mon. Wea. Rev.*, **109,** 1726–1750.

Fandry, C. B., and L. M. Leslie, 1984: A two-layer quasigeostrophic model of summer trough formation in the Australian subtropical easterlies. *J. Atmos. Sci.*, **41,** 807–818.

Garratt, J. G., 1992: *The Atmospheric Boundary Layer.* Cambridge University Press, 316 pp.

Haase, S. P., and R. K. Smith, 1989: The numerical simulation of atmospheric gravity currents. Part II: Environments with stable layers. *Geophys. Astrophys. Fluid Dyn.*, **46,** 35–51.

Hoskins, B. J., and F. P. Bretherton, 1972: Atmospheric frontogenesis models: Mathematical formulation and solution. *J. Atmos. Sci.*, **29,** 11–37.

Kepert, J. D., and R. K. Smith, 1992: A simple model of the Australian west coast trough. *Mon. Wea. Rev.*, **120,** 2042–2055.

Koch, S. E., P. B. Dorian, R. Ferrare, S. H. Melfi, W. C. Skillman, and D. Whiteman, 1991: Structure of an internal bore and dissipating gravity current as revealed by Raman lidar. *Mon. Wea. Rev.*, **119,** 857–887.

Leighton, R. M., and R. Deslandes, 1991: Monthly anticyclonicity and cyclonicity in the Australasian region: Averages for January, April, July and October. *Aust. Meteor. Mag.*, **39,** 149–154.

Miller, J. E., 1947: On the concept of frontogenesis. *J. Meteor.*, **5,** 169–171.

Mills, G. A., and R. S. Seaman, 1990: The BMRC limited area data assimilation system. *Mon. Wea. Rev.*, **118,** 1217–1237.

Noonan, J. A., and R. K. Smith, 1987: The generation of North Australian cloud lines and the "morning glory." *Aust. Meteor. Mag.*, **35,** 31–45.

Physick, W. L., and R. K. Smith, 1985: Observations and dynamics of sea breezes in northern Australia. *Aust. Meteor. Mag.*, **33,** 51–63.

——, and N. J. Tapper, 1990: A numerical study of circulations induced by a dry salt lake. *Mon. Wea. Rev.*, **118,** 1029–1042.

Reeder, M. J., 1986: The interaction of a surface cold front with a prefrontal thermodynamically well-mixed boundary layer. *Aust. Meteor. Mag.*, **34,** 137–148.

——, and R. K. Smith, 1988: On the horizontal resolution of fronts in numerical weather prediction models. *Aust. Meteor. Mag.*, **36,** 11–16.

——, and ——, 1992: Australian spring and summer cold fronts. *Aust. Meteor. Mag.*, **41,** 101–124.

——, D. Keyser, and B. D. Schmidt, 1991: Three-dimensional baroclinic instability and summertime frontogenesis in the Australian region. *Quart. J. Roy. Meteor. Soc.*, **117,** 1–28.

Reible, D. D., J. E. Simpson, and P. F. Linden, 1993: The sea breeze and gravity-current frontogenesis. *Quart. J. Roy. Meteor. Soc.*, **119,** 1–16.

Restall, W. W., and T. Shyu, 1991: A UHF wind profiling Doppler radar in a real-time application, first experiences and impressions. Preprints, *25th Conf. on Radar Meteorology,* Paris, France, Amer. Meteor. Soc., 701–704.

Rottmann, J. W., and J. E. Simpson, 1989: The formation of internal bores in the atmosphere: A laboratory model. *Quart. J. Roy. Meteor. Soc.*, **115,** 941–963.

Smith, R. K., 1988: Waves and bores in the lower atmosphere: The "morning glory" and related phenomena. *Earth Sci. Rev.*, **25,** 267–290.

——, and B. R. Morton, 1984: An observational study of northeasterly morning glory wind surges. *Aust. Meteor. Mag.*, **32,** 155–175.

——, and M. J. Reeder, 1988: On the movement and low-level structure of cold fronts. *Mon. Wea. Rev.*, **116,** 1927–1944.

——, and R. N. Ridley, 1990: Subtropical continental cold fronts. *Aust. Meteor. Mag.*, **38,** 191–200.

——, M. J. Coughlan, and J. Evans-Lopez, 1986: Southerly nocturnal wind surges and bores in northeastern Australia. *Mon. Wea. Rev.*, **114,** 1501–1518.

Whitham, G. B., 1974: *Linear and Nonlinear Waves.* Wiley, 636 pp.

Wood, I. R., and J. E. Simpson, 1984: Jumps in layered miscible fluids. *J. Fluid Mech.*, **104,** 329–342.